SLAC-PUB 7383
hep-ph/9612348
December 1996

Exact Results on $\mathcal{O}(\alpha^2)$ Single Bremsstrahlung Corrections to Low Angle Bhabha Scattering at LEP/SLC Energies

Michael Melles

Stanford Linear Accelerator Center
Stanford University, Stanford, CA 94309

Abstract

In this thesis exact results on $\mathcal{O}(\alpha^2)$ single bremsstrahlung corrections to low angle Bhabha scattering at LEP/SLC energies are given. The calculation represents the last outstanding theoretical second order subleading electroweak contribution for that process, needed to determine the experimental luminosity at second generation LEP detectors below the 0.1% precision threshold. The exact, fully differential result is obtained by employing analytical as well as computer-algebraic methods and includes terms up to $\mathcal{O}(0.05\%)$ relative to the Born cross section. The initial output of over 20,000 terms could be reduced to 90, only 18 of which are shown to be numerically relevant and for which a simple logarithmic ansatz is derived, that is in remarkable agreement with the complete answer. Strong consistency checks are performed, including Ward-Takahashi identities and tests on the right infrared limit according to the Yennie, Frautschi and Suura program. Monte Carlo results for the integrated cross section are compared with existing calculations in the leading logarithmic approximation for a chosen set of experimental cuts. The size of the missing subleading terms is found to be small but non negligible in the context of setting stringent limits on Standard Model predictions and thus its realm of validity.

To be published in Acta Physica Polonica

Research supported by the Department of Energy under grants DE-AC03-76SF00515, DE-FG05-91ER40627 and by the Deutsche Forschungsgemeinschaft (DFG)

Contents

Part I

$\mathcal{O}(\alpha)$ Corrections to $e^- + e^+ \longrightarrow e^- + e^+ + \gamma$

Chapter 1

Introduction

High precision measurements at the LEP/SLC colliders have made tremendous improvements over the last few years. At LEP, for instance, first generation detectors have measured the absolute luminosity with an accuracy of $0.3-0.5\%$ [3]. Present detectors have reached a precision below the $1pm$ threshold [3]. This level of precision opens up a wide range of new stringent constraints that can be specified not only for physics beyond the Standard Model, but also for the Higgs sector and other parameters of the electroweak theory [10]. While LEP *II* is now on line to probe the W^+, W^- aspect of the GSW-model, there is still a lot of interest in the LEP *I* energy regime of the intermediary neutral vector boson.

In general, the Z line shape is described by three parameters: M_Z, Γ_Z and σ^0 [3]. The luminosity normalizes the line shape cross section and it thus directly influences the accuracy of the σ^0 measurement. In order to determine the luminosity L, one needs to count the number of events N for a process in which the cross section σ is "known":

$$L = \frac{N}{\sigma} \tag{1.1}$$

The "known" process at LEP/SLC is low angle Bhabha scattering [18]. More than 99% of this cross section is due to t-channel photon exchange [44] and can in principle be calculated in QED with arbitrary precision. The remaining part of the cross section is due to s-channel Z, t-channel γ interference, and its relative contribution decreases with decreasing scattering angle [3].

The overall accuracy of the "known" cross section is very important for high precision measurements of Standard Model parameters since a relative luminosity error $\frac{\delta L}{L} = 10^{-3}$, for example, changes σ_0 by $42pb$ and N_ν, the number of massless neutrino generations, by 0.0075 [3]. Also $\Gamma_e \equiv \Gamma(Z \rightarrow e^+ + e^-)$ is directly affected by the precision of L since [32]

$$\Gamma_e^2 = \frac{M_Z^2 \sigma_e^0 \Gamma_Z^2}{12\pi}, \tag{1.2}$$

which is one of the main sources of our knowledge of the electroweak mixing angle [32]. It is is thus necessary to have theoretical calculations that can match the experimental accuracy below the $1pm$ mark. As can be seen from Refs. [35, 39, 40], this has not yet been achieved, although initial state s-channel $\mathcal{O}(\alpha^2)$ corrections, including two loop effects have been calculated [8]. The result of Ref. [8] for one virtual and one hard photon, however, is not suited for a Monte Carlo implementation since it was calculated in an "inclusive" way, i.e. it is not differential in the photon angles, which prohibits any adaptation to a given detector geometry. This is reflected in the form that the aspect of the theoretical uncertainty that contributes most to the present $1.6pm$ precision level is given by the missing parts of the second order subleading terms originating from the one photon bremsstrahlung process [35]. In this thesis, the exact $\mathcal{O}(\alpha)$ virtual corrections to the single hard bremsstrahlung cross section at $\sqrt{s} = M_Z$ are calculated up to the precision required in the above context, i.e. up to $\mathcal{O}(\leq 0.05\%)$. This means, for instance, that two photon exchange contributions can be neglected [34] as well as t-channel Z exchange diagrams [35]. The result is calculated in differential form and Monte Carlo [41] results then give the integrated cross section that is relevant for the theoretical prediction of the low angle Bhabha scattering cross section, needed to determine the luminosity L.
This work is structured as follows:
Chapter 2 describes the conventions and defines the notation used in this thesis. A brief section is devoted to scalar integrals and how to approach complex loop integrals in the context of using an algebraic manipulation language. It also gives an expression for the single bremsstrahlung tree level amplitude $A^{TL}_{e^-}$, which will prove to be pivotal for the final form of the exact differential result given in chapter 4.
In **chapter 3** the details of the calculation of the $\mathcal{O}(\alpha)$ virtual corrections to the single hard bremsstrahlung cross section are presented. The nature of the problem of evaluating higher order Feynman amplitudes brings with it a somewhat unavoidable technical aspect in the various sections. This chapter contains the new results presented in this work in conjunction with the appendices.
A summary of the various expressions of chapter 3 is given in **chapter 4** as the complete differential result. First numerical results are presented and discussed.
Chapters 5 and 6 are devoted to demonstrating that the presented exact differential result satisfies various internal consistency checks and has all the properties expected from general theoretical arguments.
The total cross section resulting from the differential expression in chapter 4 is obtained by means of a Monte Carlo phase space integration and numerical comparisons with other published leading log (LL) type calculations are presented in **chapter 7** for cuts similar to those used at the luminosity detector SICAL at ALEPH in LEP [36]. Also, a new approximation is derived that shows excellent agreement with the exact result and the overall size of the subleading terms is discussed.
Finally, **chapter 8** contains a summary of the results obtained in this thesis in the context of the present status of high precision radiative corrections and also concluding remarks.

Chapter 2

Basic Definitions and Identities

In this chapter the basic notations and definitions will be discussed as well as some identities that follow from the high energy limit. If nothing else is stated explicitly, the conventions of Bjorken and Drell [2] are used throughout this work. Since the overall objective of this thesis is a high precision calculation of $\mathcal{O}(\alpha^2)$ radiative corrections to a high energy process, it will prove to be very convenient to make use of the so called high energy limit, where terms of order $\frac{m_e{}^2}{-t}$ can be neglected. As a consequence of rendering the electrons (positrons) massless, their helicity will be conserved. This then leads to the very useful concept of introducing fermion helicity states [25] which are defined here by the following Dirac notation [11]:

$$|P,\lambda\rangle \equiv u_\lambda(P) = v_{-\lambda}(P) \tag{2.1}$$
$$\langle P,\lambda| \equiv \bar{u}_\lambda(P) = \bar{v}_{-\lambda}(P) \tag{2.2}$$

Eqs. 2.1, 2.2 hold for arbitrary four-momentum P with $P^2 = 0$ and u, v defined as in Ref. [2]. The normalization is fixed by demanding that

$$\langle P,\lambda|\,\gamma_\mu\,|P,\lambda\rangle = 2P_\mu \tag{2.3}$$

For two arbitrary massless four-momenta, P and Q, the following equations hold:

$$\langle P,\lambda|Q,\lambda\rangle = 0\,;\,\langle P,-\lambda|P,\lambda\rangle = 0\,;\,\not{P}\,|P,\lambda\rangle = 0 \tag{2.4}$$
$$\langle P,-\lambda|Q,\lambda\rangle = -\langle Q,-\lambda|P,\lambda\rangle\,;\,\not{P} = |P,\lambda\rangle\langle P,\lambda| + |P,-\lambda\rangle\langle P,-\lambda| \tag{2.5}$$
$$\langle P,-\lambda|Q,\lambda\rangle\,\langle Q,\lambda|P,-\lambda\rangle = 2PQ = (P+Q)^2 \tag{2.6}$$

Furthermore, for arbitrary four-momenta k_i:

$$\langle P,\lambda|\not{k}_1 \ldots \not{k}_n |Q,\lambda\rangle = \langle Q,-\lambda|\not{k}_n \ldots \not{k}_1 |P,-\lambda\rangle \quad ,n \text{ odd} \tag{2.7}$$

$$\langle P,-\lambda|\not{k}_1 \ldots \not{k}_n |Q,\lambda\rangle = -\langle Q,-\lambda|\not{k}_n \ldots \not{k}_1 |P,\lambda\rangle \quad ,n \text{ even} \tag{2.8}$$

An important identity that will be used extensively is the Fierz-identity [19] and holds for arbitrary spinors $|A,\lambda\rangle$, $|B,\lambda'\rangle$, $|C,\mu\rangle$ and $|D,\mu'\rangle$:

$$\langle A,\lambda|\gamma_\nu|B,\lambda\rangle\langle C,\mu|\gamma^\nu|D,\mu\rangle = 2\langle A,\lambda|X,-\lambda\rangle\langle Y,-\lambda|B,\lambda\rangle , \tag{2.9}$$

where

$$(X,Y) = \begin{cases} (C,D) & ,\lambda=\mu \\ (D,C) & ,\lambda=-\mu \end{cases} \tag{2.10}$$

It is sometimes convenient to simply write

$$\langle P,Q\rangle_\lambda \equiv \langle P,-\lambda|Q,\lambda\rangle \tag{2.11}$$

The "magic" polarization vector of Xu, Zhang and Chang is given by [46] :

$$\varepsilon_\mu(K,h,\rho) = \frac{\rho}{\sqrt{2}}\frac{\langle h,-\rho|\gamma_\mu|K,-\rho\rangle}{\langle h,K\rangle_\rho} , \tag{2.12}$$

where K is the photon four-momentum, ρ its polarization and h a reference momentum with $h^2 = 0$. Choosing h amounts to a gauge choice and this freedom can be exploited to greatly simplify calculations with bremsstrahlung effects [11]. If the incoming electron has a four-momentum P, the outgoing one a four-momentum Q and if its helicity is denoted by λ, the "magic" choice in the present calculation turns out to be :

$$h = \begin{cases} P & ,\lambda=\rho \\ Q & ,\lambda=-\rho \end{cases} \tag{2.13}$$

For completeness, there are three other helicity dependent four-momenta used in this work, $h', \widehat{h}$ and $\widehat{h'}$, where analogously for the positron line

$$h' = \begin{cases} P' & ,\lambda'=\rho \\ Q' & ,\lambda'=-\rho \end{cases} \tag{2.14}$$

$\widehat{h}$ and $\widehat{h'}$ denote the helicity flipped choices of h and h' respectively.
It is also helpful to give $\not{\varepsilon}$ explicitly, since it is the object appearing in expressions for Feynman amplitudes :

$$\not{\varepsilon} = \frac{\rho\sqrt{2}}{\langle h,K\rangle_\rho}\left(|K,-\rho\rangle\langle h,-\rho| + |h,\rho\rangle\langle K,\rho|\right) \tag{2.15}$$

As an application, the "magic" properties of ε_μ are used in proving the following important identity for $\lambda = \rho$:

$$
\begin{aligned}
0 \;=\; & PQ\,\langle Q',\lambda'|\not{\varepsilon}\,|P',\lambda'\rangle\,\langle Q,\lambda|\not{K}\,|P,\lambda\rangle \;- \\
& Q\varepsilon\;\langle Q',\lambda'|\not{P}\,|P',\lambda'\rangle\,\langle Q,\lambda|\not{K}\,|P,\lambda\rangle \;+ \\
& PK\,Q\varepsilon\,\langle Q',\lambda'|\,\gamma_\mu\,|P',\lambda'\rangle\,\langle Q,\lambda|\,\gamma^\mu\,|P,\lambda\rangle
\end{aligned}
\tag{2.16}
$$

Eq. 2.16 can be proved by observing that

$$
PK\,\langle Q,\lambda|\,\gamma^\mu\,|P,\lambda\rangle \;=\; P^\mu\,\langle Q,\lambda|\not{K}\,|P,\lambda\rangle \;-\; \frac{1}{2}\,\langle Q,\lambda|\not{P}\,\gamma^\mu\not{K}\,|P,\lambda\rangle \tag{2.17}
$$

$$
PQ\,\langle Q,\lambda|\not{K}\,|P,\lambda\rangle \;=\; \frac{1}{2}\,\langle Q,\lambda|\not{P}\not{Q}\not{K}\,|P,\lambda\rangle \tag{2.18}
$$

Thus, it remains to be shown that

$$
\begin{aligned}
0 \;=\; & \langle Q',\lambda'|\not{\varepsilon}\,|P',\lambda'\rangle\,\langle Q,\lambda|\not{P}\not{Q}\not{K}\,|P,\lambda\rangle \;- \\
& Q\varepsilon\,\langle Q',\lambda'|\,\gamma_\mu\,|P',\lambda'\rangle\,\langle Q,\lambda|\not{P}\,\gamma^\mu\not{K}\,|P,\lambda\rangle\,,
\end{aligned}
\tag{2.19}
$$

which follows from the transversality condition $\varepsilon K = 0$ and the "magic" properties

$$
\not{\varepsilon}\,|P,\lambda\rangle \;=\; 0 \;\;\&\;\; \{\not{P},\not{\varepsilon}\} \;=\; 0 \qquad ,\lambda = \rho \tag{2.20}
$$

An analogous identity holds for $\lambda = -\rho$ and reads:

$$
\begin{aligned}
0 \;=\; & PQ\,\langle Q',\lambda'|\not{\varepsilon}\,|P',\lambda'\rangle\,\langle Q,\lambda|\not{K}\,|P,\lambda\rangle \;- \\
& P\varepsilon\;\langle Q',\lambda'|\not{Q}\,|P',\lambda'\rangle\,\langle Q,\lambda|\not{K}\,|P,\lambda\rangle \;+ \\
& QK\,P\varepsilon\,\langle Q',\lambda'|\,\gamma_\mu\,|P',\lambda'\rangle\,\langle Q,\lambda|\,\gamma^\mu\,|P,\lambda\rangle
\end{aligned}
\tag{2.21}
$$

Eq. 2.21 can be directly obtained from Eq. 2.16 through the crossing rule:

$$
P \;\leftrightarrow\; -Q \;\;,\;\; \lambda \;\rightarrow\; -\lambda \tag{2.22}
$$

The usefulness of the helicity dependent spinor notations 2.13, 2.14 can be exemplified by stating the identities 2.16, 2.21 through a helicity independent notation:

$$
\begin{aligned}
0 \;=\; & h\widehat{h}\,\langle Q',\lambda'|\not{\varepsilon}\,|P',\lambda'\rangle\,\langle Q,\lambda|\not{K}\,|P,\lambda\rangle \;- \\
& \widehat{h}\varepsilon\;\langle Q',\lambda'|\not{h}\,|P',\lambda'\rangle\,\langle Q,\lambda|\not{K}\,|P,\lambda\rangle \;+ \\
& hK\,\widehat{h}\varepsilon\,\langle Q',\lambda'|\,\gamma_\mu\,|P',\lambda'\rangle\,\langle Q,\lambda|\,\gamma^\mu\,|P,\lambda\rangle
\end{aligned}
\tag{2.23}
$$

Note in particular that the polarization vector ε_μ in 2.12 is invariant under the transformation 2.22, which relates initial to final state electron-line radiation

and thus insures that the same polarization vector be used for one line in each helicity case.
The following definitions will also be extensively used throughout this work, where the four-momenta are those of 2.13 and 2.14:

$$\alpha \equiv 2PK = -(P-K)^2 \quad (2.24)$$
$$\beta \equiv 2QK = (Q+K)^2 \quad (2.25)$$
$$s \equiv 2PP' = (P+P')^2 \quad (2.26)$$
$$s' \equiv 2QQ' = (Q+Q')^2 \quad (2.27)$$
$$t \equiv -2PQ = (P-Q)^2 \quad (2.28)$$
$$t' \equiv -2P'Q' = (P'-Q')^2 \quad (2.29)$$

It should be mentioned that the fine structure constant $\alpha = \frac{e^2}{4\pi} = \frac{1}{137}$ will not appear explicitly in equations in this work unless specifically mentioned in order to avoid confusing notation.
The t-channel process, as shown in Fig. 2.1, also allows for Z-boson exchange in the present calculation, mainly to be able to incorporate s-channel Z, t-channel γ interference and, at a later stage, to possibly allow for wide-angle applications. The propagator $G_{\lambda,\lambda'}(t')$ is then given by [28]:

$$G_{\lambda,\lambda'}(t') = \frac{1}{t'} + \frac{[(1-\lambda) - 4sin^2\theta_w][(1-\lambda') - 4sin^2\theta_w]}{4sin^2 2\theta_w (t' - {M_Z}^2)}, \quad (2.30)$$

where θ_w denotes the weak mixing angle and M_Z the mass of the intermediary Z-boson [20]. In the s-channel a correction coming from the imaginary part of the self-energy correction [28] needs to be taken into account and leads to the replacement rule ${M_Z}^2 \longrightarrow {M_Z}^2 - is\frac{\Gamma_Z}{M_Z}$, where Γ_Z is the width of the Z-boson.

2.1 Scalar Integrals

All results that are given below involving loop integrals are expressed in terms of so called scalar integrals, i.e. four-dimensional integrals over Minkowski space with no tensor-structure in the numerators. The analytic solutions of integrals of this type have long been known in the literature [17] and recently, a new way of numerically implementing these results in a more stable way has been proposed [13]. The results of Ref. [13] are those that have been used in this work to calculate scalar integrals by means of a numerical package called *ff*, as well as their reduction scheme, which decomposes tensor integrals into a linear combination of the easier scalar integrals. Wherever possible, the package results have been compared to known analytic results in certain limits [17, 31] and have shown very good agreement. The reduction scheme, implemented in the algebraic computer-language FORM [13], has also passed all tests that were applied to it with relatively simple test-cases. It is essential for a numerical

analysis that the algorithms, especially for the more complicated scalar integrals with three and four denominators, are reliable and indicate situations where the required cancelations become too involved to be handled within a given level of accuracy. This is one of the most important advantages the *ff*-package possesses, where roughly 80% of the programmed code ($\approx$ 50000 lines) is devoted to just that [12]. The scalar integrals used in the present calculation are defined as follows:

$$X_0^k \equiv \frac{1}{i\pi^2}\int \frac{\mu^\epsilon\, d^n l}{(l^2-m_1{}^2)((l+p_1)^2-m_2{}^2)...((l+p_1+...+p_{k-1})^2-m_k{}^2)+i\epsilon} \tag{2.31}$$

Throughout this work only scalar integrals up to $k = 4$ will be necessary and are going to be denoted by

$$X_0^1 \equiv A_0(m_1) \tag{2.32}$$
$$X_0^2 \equiv B_0(p_1{}^2, m_1, m_2) \tag{2.33}$$
$$X_0^3 \equiv C_0(p_1{}^2, p_2{}^2, (p_1+p_2)^2, m_1, m_2, m_3) \tag{2.34}$$
$$X_0^4 \equiv D_0(p_1{}^2, p_2{}^2, p_3{}^2, p_4{}^2, (p_3+p_4)^2, (p_1+p_4)^2, m_1, m_2, m_3, m_4) \tag{2.35}$$

It should be noted that, as suggested by the notation in Eq. 2.31, the scalar integrals 2.32, 2.33 are defined through the n-dimensional regularization method [27, 21]. The choice of the scale μ should not affect any result. In order to write Eq. 2.31 in an easy to recognize manner for arbitrary k, all momenta p_i are assumed to be incoming in a Feynman-diagram. For the calculation of $\mathcal{O}(\alpha^2)$ single bremsstrahlung corrections in this work, however, all physically outgoing particles will also be denoted by outgoing four-momenta, such that the scalar product of incoming with outgoing momenta will always be positive. Since massless spinors are used in this thesis, all terms homogeneous in m_e will be dropped out of the expressions derived below. The masses, however, will be kept as regulators of "unphysical" collinear divergences inside the scalar integrals.

2.2 Complex Loop Integrals and Bilinear Covariants

When using algebraic manipulation languages to calculate higher order Feynman diagrams, it is important to reduce the sometimes very involved matrix expressions in numerators of the resulting integrals. Since these terms will eventually be evaluated between spinors, it is desirable to reduce strings of Dirac gamma matrices – up to seven in integrals that will be treated in chapter 3 – to terms multiplying bilinear covariants [2]. The transformation behaviour of the various basis terms is that of a scalar (1), a pseudoscalar (γ_5), a vector (γ_μ), an axial-vector ($\gamma_5\gamma_\mu$) and that of a second rank tensor ($\sigma_{\mu\nu} \equiv \frac{i}{2}[\gamma_\mu, \gamma_\nu]$). Expanding an arbitrary string of slashed four-vectors, $G \equiv \not{a}_1 ... \not{a}_n$, yields:

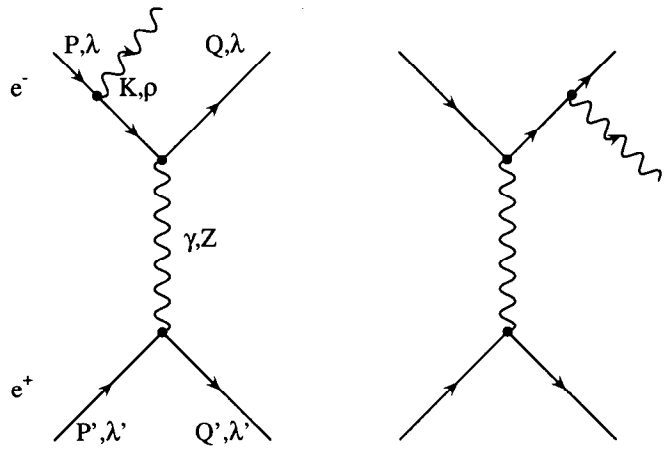

Figure 2.1: The t-channel tree level Feynman diagrams contributing to the $\mathcal{O}(\alpha)$ single bremsstrahlung cross section for initial and final state electron line emission.

$$\begin{aligned} G &= \frac{1}{4}Tr(G)1 + \frac{1}{4}Tr(\gamma_5 G)\gamma_5 + \frac{1}{4}Tr(\gamma_\mu G)\gamma^\mu \\ &\quad -\frac{1}{4}Tr(\gamma_5\gamma_\mu G)\gamma_5\gamma^\mu + \frac{1}{8}Tr(\sigma_{\mu\nu}G)\sigma^{\mu\nu} \end{aligned} \tag{2.36}$$

It can be easily checked that if G is one of the stated basis vectors, Eq. 2.36 holds in each case. The use of γ_5 can be avoided in n-dimensions, but the algebra in the end always assumes that the spinor space remains four-dimensional. The reduction 2.36 also allows the application of the entire spinology that was described in the beginning of this chapter, since the terms in 2.36 are easily evaluated between spinors. Ref. [24] contains a program written in FORM that produces the presented reduction in n-dimensions and is employed in most of the other routines used in this thesis.

2.3 The Tree Level Single Bremsstrahlung Amplitudes

The $\mathcal{O}(\alpha)$ t-channel single bremsstrahlung electron-line emission amplitudes are shown in Fig. 2.1. In the high-energy limit $\frac{{m_e}^2}{-t} \ll 1$, one can legitimately make use of the massless spinor formulation described in chapter 2 and of the helicity conserving "magic" polarization-vector in Eq. 2.12. The tree-level amplitude, from now on denoted by $A^{TL}_{e^-}$, can, for initial state electron-line emission, Fig. 2.1, be expressed as

$$
\begin{aligned}
A_{e^-}^{TL} &= \frac{ie^3}{-2PK}\langle Q',\lambda'|\gamma_\mu|P',\lambda'\rangle G_{\lambda,\lambda'}(t')\times \\
&\quad \langle Q,\lambda|\gamma^\mu(\not{P}-\not{K})\not{\varepsilon}|P,\lambda\rangle \qquad (2.37)\\
&= \frac{ie^3 G_{\lambda,\lambda'}(t')\delta_{\lambda,-\rho}}{\langle K,P\rangle_\lambda\langle K,P\rangle_{-\lambda}}\,[\,2P\varepsilon\langle Q',\lambda'|\gamma_\mu|P',\lambda'\rangle\langle Q,\lambda|\gamma^\mu|P,\lambda\rangle \\
&\quad +\ 2\,\langle Q',\lambda'|\not{\varepsilon}|P',\lambda'\rangle\langle Q,\lambda|\not{K}|P,\lambda\rangle\,] \qquad (2.38)\\
&= \frac{ie^3\sqrt{8}\rho G_{\lambda,\lambda'}(t')\delta_{\lambda,-\rho}}{\langle K,P\rangle_\lambda\langle K,P\rangle_{-\lambda}\langle h,K\rangle_\rho}\times \\
&\quad \Big[\ \langle Q,P\rangle_{-\lambda}\langle P,K\rangle_\lambda\begin{cases}\langle Q',Q\rangle_{-\lambda'}\langle P,P'\rangle_{\lambda'} & ,\lambda=\lambda'\\ \langle Q',P\rangle_{-\lambda'}\langle Q,P'\rangle_{\lambda'} & ,\lambda=-\lambda'\end{cases}\\
&\quad +\langle Q,K\rangle_{-\lambda}\langle K,P\rangle_\lambda\begin{cases}\langle Q',Q\rangle_{-\lambda'}\langle K,P'\rangle_{\lambda'} & ,\lambda=\lambda'\\ \langle Q',K\rangle_{-\lambda'}\langle Q,P'\rangle_{\lambda'} & ,\lambda=-\lambda'\end{cases}\Big]\\
&= \frac{ie^3\sqrt{8}\rho G_{\lambda,\lambda'}(t')\delta_{\lambda,-\rho}}{\langle P,K\rangle_{-\lambda}\langle h,K\rangle_\rho}\times \\
&\quad \Big[\ \langle Q,P\rangle_{-\lambda}\begin{cases}\langle Q',Q\rangle_{-\lambda'}\langle P,P'\rangle_{\lambda'} & ,\lambda=\lambda'\\ \langle Q',P\rangle_{-\lambda'}\langle Q,P'\rangle_{\lambda'} & ,\lambda=-\lambda'\end{cases}\\
&\quad -\langle Q,K\rangle_{-\lambda}\begin{cases}\langle Q',Q\rangle_{-\lambda'}\langle K,P'\rangle_{\lambda'} & ,\lambda=\lambda'\\ \langle Q',K\rangle_{-\lambda'}\langle Q,P'\rangle_{\lambda'} & ,\lambda=-\lambda'\end{cases}\Big]\\
&= \frac{ie^3\sqrt{8}\rho G_{\lambda,\lambda'}(t')\delta_{\lambda,-\rho}}{\langle P,K\rangle_\rho\langle h,K\rangle_\rho}\times \\
&\quad \begin{cases}\langle Q',Q\rangle_\rho(\langle Q,P\rangle_{-\lambda}\langle P,P'\rangle_\lambda-\langle Q,K\rangle_{-\lambda}\langle K,P'\rangle_\lambda) & ,\lambda=\lambda'\\ \langle Q,P'\rangle_\rho(\langle Q,P\rangle_{-\lambda}\langle Q',P\rangle_\lambda-\langle Q,K\rangle_{-\lambda}\langle Q',K\rangle_\lambda) & ,\lambda=-\lambda'\end{cases}\\
&= \frac{ie^3\sqrt{8}\rho G_{\lambda,\lambda'}(t')\delta_{\lambda,-\rho}}{\langle P,K\rangle_\rho\langle h,K\rangle_\rho}\begin{cases}\langle Q',Q\rangle_\rho\langle Q,Q'\rangle_{-\lambda}\langle Q',P'\rangle_\lambda & ,\lambda=\lambda'\\ \langle Q,P'\rangle_\rho\langle Q,P'\rangle_{-\lambda}\langle P',Q'\rangle_\lambda & ,\lambda=-\lambda'\end{cases}\\
&= ie^3\sqrt{8}\,\lambda' G_{\lambda,\lambda'}(t')\,\frac{\langle h',\widehat{h'}\rangle_{-\rho}(\langle h,h'\rangle_\rho)^2}{\langle h,K\rangle_\rho\langle\widehat{h},K\rangle_\rho}\,, \qquad (2.39)
\end{aligned}
$$

where the properties of ε_μ of Eq. 2.12, four-momentum conservation and the Fierz-identity Eq. 2.9 were used. Eq. 2.39, derived for a specific electron-photon helicity correlation, holds in fact for both helicity cases. This was achieved by using the helicity dependent h-spinors of chapter 2. Although Eq. 2.39 represents the numerically most stable form for $A_{e^-}^{TL}$, there is another way of writing 2.37 by means of the identity 2.23 which will prove to be very useful in the calculation at a later point and is indeed the main application of 2.23:

$$A_{e^-}^{TL} = \frac{ie^3}{\widehat{hK}} G_{\lambda,\lambda'}(t') [\frac{\rho\lambda t - 2hK}{t} \langle Q', \lambda' | \gamma_\mu | P', \lambda' \rangle \langle Q, \lambda | \gamma^\mu | P, \lambda \rangle + \frac{2}{t} \langle Q', \lambda' | \not{p} | P', \lambda' \rangle \langle Q, \lambda | \not{K} | P, \lambda \rangle] \widehat{h\varepsilon} \quad (2.40)$$

Eq. 2.40 will play an important role in separating out the "true" tree-level part of the complete $\mathcal{O}(\alpha^2)$ internal emission calculation in chapter 3.3; see also Ref. [24].

Chapter 3

The $\mathcal{O}(\alpha^2)$ Single Bremsstrahlung Amplitudes

This chapter is devoted to describing in detail the steps of the second order calculation. While a lot of analytical work is presented, all occuring loop integrals were evaluated in the appendices of Ref. [24] with the algebraic manipulation language FORM. It is assumed from this point on that all UV-divergences will be properly taken care of by the appropriate counter terms in the Lagrangian such that in the on-shell renormalization scheme $-e$ and m_e correspond to the physically observable charge and mass of the electron respectively.
Employing standard Feynman techniques [21, 42] gives 18 electron line emission graphs for the desired level of precision in the previously described context (compare with chapter 1). The single bremsstrahlung amplitudes contributing to $\mathcal{O}(\alpha^2)$ radiative corrections to the low angle Bhabha cross section are listed in Fig. 3.1 for t-channel electron-line emission. Positron-line emission can be obtained from these amplitudes through crossing relations:

$$P \longleftrightarrow -Q' \tag{3.1}$$
$$P' \longleftrightarrow -Q \tag{3.2}$$
$$\lambda \longrightarrow -\lambda \tag{3.3}$$

A crossing rule can also be used to calculate the initial state s-channel contribution by applying 3.2 to the electron-line t-channel calculation. The s-channel final state contribution is attained by employing 3.1 and 3.3 to the expressions corresponding to the diagrams shown in Fig. 3.1. All vacuum polarization graphs that would in principle also belong to this class of diagrams are explicitly omitted here, since they are already included in BHLUMI4.01 [35].

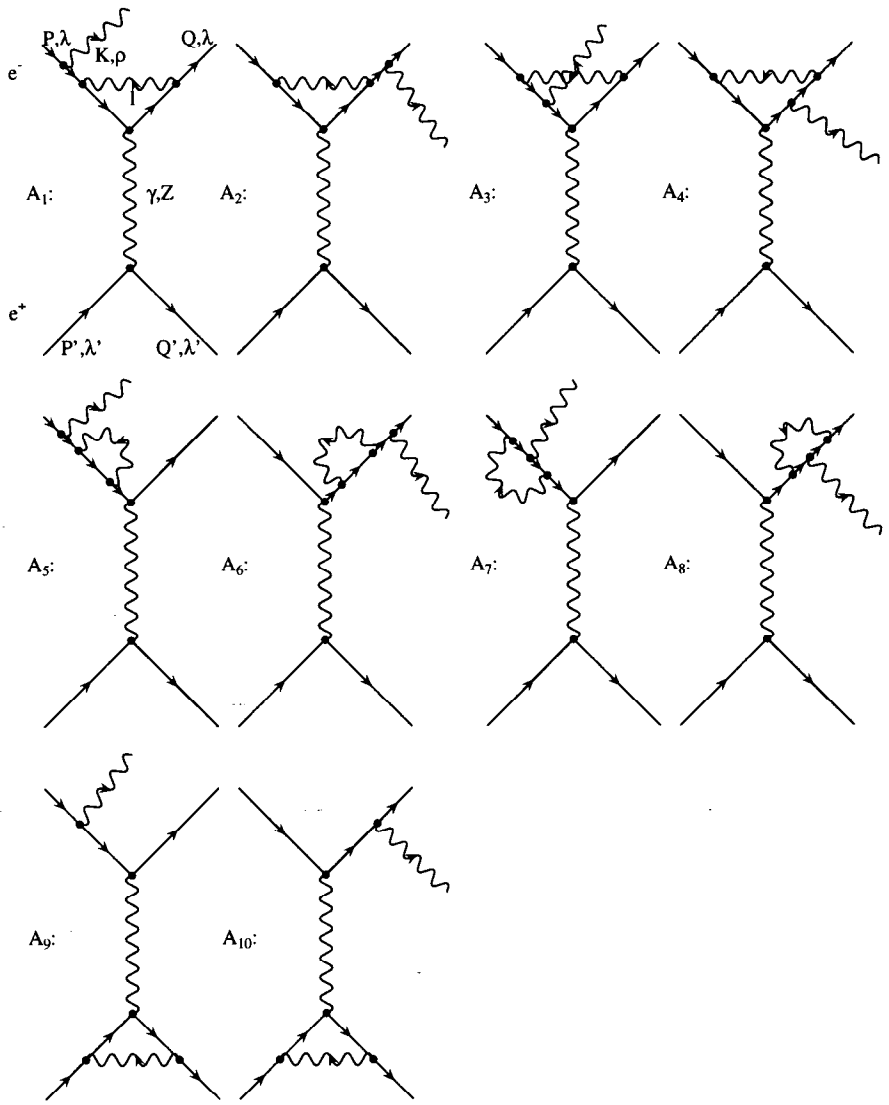

Figure 3.1: The one particle t-channel exchange Feynman diagrams, modulo vacuum polarization graphs, for initial and final state electron line emission that give a nonzero contribution to the $\mathcal{O}(\alpha^2)$ single bremsstrahlung cross section after renormalization is carried out in the chosen on-shell scheme. Also Z-exchange can be included.

Following the notation of Fig. 3.1 the various graphs translate into the amplitudes given by the expressions listed below. It should be noted that the Feynman gauge [23, 42] was picked to arrive at the following representation. The divergent integrals are regularized by means of the n-dimensional regularization technique.

$$A_1 = \frac{e^5}{(2\pi)^4}\langle Q',\lambda'|\gamma_\mu|P',\lambda'\rangle G_{\lambda,\lambda'}(t')\times \int \frac{\mu^\epsilon d^n l}{-2PK}\frac{\langle Q,\lambda|\gamma_\nu(\not l+\not Q)\gamma^\mu(\not l+\not P-\not K)\gamma^\nu(\not P-\not K)\not\epsilon|P,\lambda\rangle}{(l^2-m_0{}^2)((l+P-K)^2-m_e{}^2)((l+Q)^2-m_e{}^2)+i\epsilon} \tag{3.4}$$

$$A_2 = \frac{e^5}{(2\pi)^4}\langle Q',\lambda'|\gamma_\mu|P',\lambda'\rangle G_{\lambda,\lambda'}(t')\times \int \frac{\mu^\epsilon d^n l}{2QK}\frac{\langle Q,\lambda|\not\epsilon(\not Q+\not K)\gamma_\nu(\not l+\not Q+\not K)\gamma^\mu(\not l+\not P)\gamma^\nu|P,\lambda\rangle}{(l^2-m_0{}^2)((l+P)^2-m_e{}^2)((l+Q+K)^2-m_e{}^2)+i\epsilon} \tag{3.5}$$

$$A_3 = \frac{e^5}{(2\pi)^4}\langle Q',\lambda'|\gamma_\mu|P',\lambda'\rangle G_{\lambda,\lambda'}(t')\times \int \frac{d^4l\langle Q,\lambda|\gamma_\nu(\not l+\not Q)\gamma^\mu(\not l+\not P-\not K)\not\epsilon(\not l+\not P)\gamma^\nu|P,\lambda\rangle}{(l^2-m_0{}^2)((l+P)^2-m_e{}^2)((l+P-K)^2-m_e{}^2)((l+Q)^2-m_e{}^2)+i\epsilon} \tag{3.6}$$

$$A_4 = \frac{e^5}{(2\pi)^4}\langle Q',\lambda'|\gamma_\mu|P',\lambda'\rangle G_{\lambda,\lambda'}(t')\times \int \frac{d^4l\langle Q,\lambda|\gamma_\nu(\not l+\not Q)\not\epsilon(\not l+\not Q+\not K)\gamma^\mu(\not l+\not P)\gamma^\nu|P,\lambda\rangle}{(l^2-m_0{}^2)((l+P)^2-m_e{}^2)((l+Q+K)^2-m_e{}^2)((l+Q)^2-m_e{}^2)+i\epsilon} \tag{3.7}$$

$$A_5 = \frac{e^5}{(2\pi)^4}\langle Q',\lambda'|\gamma_\mu|P',\lambda'\rangle G_{\lambda,\lambda'}(t')\times \langle Q,\lambda|\gamma^\mu\frac{\not P-\not K}{-2PK}\int\mu^\epsilon d^n l\frac{\gamma_\nu(\not l+\not P-\not K)\gamma^\nu}{(l^2-m_0{}^2)((l+P-K)^2-m_e{}^2)+i\epsilon}\frac{\not P-\not K}{-2PK}\not\epsilon|P,\lambda\rangle \tag{3.8}$$

$$A_6 = \frac{e^5}{(2\pi)^4}\langle Q',\lambda'|\gamma_\mu|P',\lambda'\rangle G_{\lambda,\lambda'}(t')\times \langle Q,\lambda|\not\epsilon\frac{\not Q+\not K}{2QK}\int\mu^\epsilon d^n l\frac{\gamma_\nu(\not l+\not Q+\not K)\gamma^\nu}{(l^2-m_0{}^2)((l+Q+K)^2-m_e{}^2)+i\epsilon}\frac{\not Q+\not K}{2QK}\gamma^\mu|P,\lambda\rangle \tag{3.9}$$

$$A_7 = \frac{e^5}{(2\pi)^4}\langle Q',\lambda'|\gamma_\mu|P',\lambda'\rangle G_{\lambda,\lambda'}(t')\times \langle Q,\lambda|\gamma^\mu\frac{\not P-\not K}{-2PK}\int\frac{\mu^\epsilon d^n l\,\gamma_\nu(\not l+\not P-\not K)\not\epsilon(\not l+\not P)\gamma^\nu}{(l^2-m_0{}^2)((l+P)^2-m_e{}^2)((l+P-K)^2-m_e{}^2)+i\epsilon}|P,\lambda\rangle \tag{3.10}$$

$$A_8 = \frac{e^5}{(2\pi)^4}\langle Q',\lambda'|\gamma_\mu|P',\lambda'\rangle G_{\lambda,\lambda'}(t')\times$$
$$\langle Q,\lambda|\int\frac{\mu^\epsilon d^n l\,\gamma_\nu(\not l+\not Q)\not\epsilon(\not l+\not Q+\not K)\gamma^\nu}{(l^2-m_0{}^2)((l+Q)^2-m_e{}^2)((l+Q+K)^2-m_e{}^2)+i\epsilon}\frac{\not Q+\not K}{2QK}\gamma^\mu|P,\lambda\rangle \tag{3.11}$$

$$A_9 = \frac{e^5}{(2\pi)^4}\langle Q,\lambda|\gamma_\mu\frac{\not P-\not K}{-2PK}\not\epsilon|P,\lambda\rangle G_{\lambda,\lambda'}(t')\times$$
$$\int\frac{\mu^\epsilon d^n l\langle Q',\lambda'|\gamma_\nu(\not l+\not Q')\gamma^\mu(\not l+\not P')\gamma^\nu|P',\lambda'\rangle}{(l^2-m_0{}^2)((l+P')^2-m_e{}^2)((l+Q')^2-m_e{}^2)+i\epsilon} \tag{3.12}$$

$$A_{10} = \frac{e^5}{(2\pi)^4}\langle Q,\lambda|\not\epsilon\frac{\not Q+\not K}{2QK}\gamma_\mu|P,\lambda\rangle G_{\lambda,\lambda'}(t')\times$$
$$\int\frac{\mu^\epsilon d^n l\langle Q',\lambda'|\gamma_\nu(\not l+\not Q')\gamma^\mu(\not l+\not P')\gamma^\nu|P',\lambda'\rangle}{(l^2-m_0{}^2)((l+P')^2-m_e{}^2)((l+Q')^2-m_e{}^2)+i\epsilon} \tag{3.13}$$

The following sections of this chapter will now go about solving the integrals appearing in Eqs. 3.4 – 3.13 and give concise expressions for the corresponding amplitudes.

3.1 Vertex Corrections

The name "vertex corrections" to the $\mathcal{O}(\alpha)$ single bremsstrahlung cross section implies that some kind of a factorization takes place, that separates the lower order amplitudes from the additional virtual corrections. This, however, is not true in general and only holds in this calculation for A_1, A_2, A_9 and A_{10} because of the application of the high energy approximation and the use of the "magic" polarization vector 2.15 and the "magic" choices given in Eqs. 2.13 and 2.14. The graphs calculated in this section include amplitudes 3.4, 3.5, 3.10, 3.11, 3.12 and 3.13. For the amplitudes A_7 and A_8, the described factorization does not take place despite the tools mentioned above. It still will be useful in this case to use the broad headline "vertex correction" because of two reasons:

The result for A_7 and A_8 is completely determined by form factors derived in this section and secondly, the terms not proportional to the lower order, tree level, amplitude turn out to be canceled exactly by a contribution contained in the rather complicated expression for A_3 and A_4, to be discussed in section 3.3. This circumstance will insure that all leading and subleading contributions will be concentrated in the factorized part of the complete answer.

All results employ the on-shell renormalization scheme, i.e. they are renormalized such that the vertex correction contribution vanishes if both fermion legs are on the mass-shell and for zero four-momentum transfer.

3.1.1 Scalar Integrals

The Scalar integrals, in terms of which the following results of the various amplitudes are given, are defined in this section as follows:

$$
\begin{aligned}
B_{12}^{\alpha} &= B_0({m_e}^2-\alpha; m_0, m_e) && (3.14)\\
B_{23} &= B_0(2{m_e}^2+t'; m_e, m_e) && (3.15)\\
B_{23}^{0} &= B_0({m_0}^2; m_e, m_e) && (3.16)\\
C_{123}^{\alpha} &= C_0({m_e}^2-\alpha, 2{m_e}^2+t', {m_e}^2; m_0, m_e, m_e) && (3.17)\\
C_{1230} &= C_0({m_e}^2, {m_0}^2, {m_e}^2, m_0, m_e, m_e) && (3.18)
\end{aligned}
$$

It must be emphasized that the notation for scalar integrals in 3.14 – 3.18 only refers to loop integrals with no more than three internal propagators. This was done in order to have agreement with the notation implicitly employed by FORM in the appendices of Ref. [24].
Eq. 3.18 is somewhat special among the integrals denoted above in that it can be expressed analytically and without renormalization and scale dependence:

$$
\begin{aligned}
C_{1230} &= \frac{1}{i\pi^2}\int d^4l \frac{1}{(l^2-{m_0}^2)(l^2+2lP)^2+i\epsilon}\\
&= \frac{2}{i\pi^2}\int d^4l \int_0^1 dx \frac{x}{(l^2+2lPx-{m_0}^2(1-x)+i\epsilon)^3}\\
&= -\int_0^1 dx \frac{x}{{m_e}^2x^2-{m_0}^2x+{m_0}^2+i\epsilon}\\
&= -\frac{1}{2{m_e}^2} ln({m_e}^2x^2-{m_0}^2x+{m_0}^2+i\epsilon)\Big|_0^1\\
&= {m_e}^{-2}\, ln\,\frac{m_0}{m_e}\,, && (3.19)
\end{aligned}
$$

where standard Feynman parameters [42, 21], integral tables [14] and formulas for integrals over four-dimensional Minkowski space [42, 21, 27] were used. In addition it follows from 3.18 that $P^2 = {m_e}^2$, so that only masses are parameters of this integral. The significance of 3.19 here is merely a notational one. It means that ${m_e}^2 C_{1230}$-terms are actually of order $\mathcal{O}({m_e}^0)$ and need to be taken into account; it also is IR-divergent, which implies the possibility of a strong analytical check of the expected limit for $m_0 \to 0$; see chapter 5 for an analysis of this problem. The same behaviour with respect to a possible ${m_e}^{-2}$ dependence is not given for the other integrals listed. Dimensional reasons exclude it for A_0 and B_0 functions and numerical checks for the other integrals in the regime where products of four-momenta are much larger than ${m_e}^2$.

3.1.2 The Vertex Function

The vertex function $\Gamma_\delta^\mu((P-Q)^2, P^2, Q^2)$ is given by the integral:

$$\Gamma_o^\mu = \frac{1}{i\pi^2}\int \mu^\epsilon d^n l \frac{\gamma_\nu(\not l+\not Q+m_e)\gamma^\mu(\not l+\not P+m_e)\gamma^\nu}{(l^2-{m_0}^2)((l+P)^2-{m_e}^2)((l+Q)^2-{m_e}^2)+i\epsilon} \qquad (3.20)$$

The numerator of the integral 3.20 can be simplified by means of standard Dirac-algebra manipulations as follows:

$$\begin{aligned}
& \gamma_\nu(\not l+\not Q+m_e)\gamma^\mu(\not l+\not P+m_e)\gamma^\nu \\
= \;& \gamma_\nu(\not l+\not Q)\gamma^\mu(\not l+\not P)\gamma^\nu + m_e\gamma_\nu\gamma^\mu(\not l+\not P)\gamma^\nu + m_e\gamma_\nu(\not l+\not Q)\gamma^\mu\gamma^\nu \\
& +{m_e}^2\gamma_\nu\gamma^\mu\gamma^\nu \\
= \;& -2(\not l+\not P)\gamma^\mu(\not l+\not Q) + 4m_e(l+P)^\mu + 4m_e(l+Q)^\mu - 2{m_e}^2\gamma^\nu \\
= \;& -2((-\gamma^\mu(\not l+\not P) + 2(l+P)^\mu)(\not l+\not Q) + (m_e - terms) \\
= \;& -4(\not l+\not Q)(l+P)^\mu + 2\gamma^\mu(-(\not l+\not Q)(\not l+\not P) + 2(l+P)(l+Q)) \\
& +(m_e - terms) \\
= \;& -4(\not l+\not Q)(l+P)^\mu + 4\gamma^\mu(l+P)(l+Q) + 2((\not l+\not Q)\gamma^\mu \\
& -2(l+Q)^\mu)(\not l+\not P) + (m_e - terms) \\
= \;& 2(\not l+\not Q)\gamma^\mu(\not l+\not P) + 4\gamma^\mu(l+P)(l+Q) - 4(l+P)^\mu(\not l+\not Q) \\
& -4(l+Q)^\mu(\not l+\not P) + (m_e - terms) \\
= \;& 2(\not l+\not Q-m_e)\gamma^\mu(\not l+\not P-m_e) + 2m_e\gamma^\mu(\not l+\not P) + 2m_e(\not l+\not Q)\gamma^\mu \\
& +4\gamma^\mu(l+P)(l+Q) - 4(l+P)^\mu(\not l+\not Q) - 4(l+Q)^\mu(\not l+\not P) \\
& +4m_e(l+P)^\mu + 4m_e(l+Q)^\mu - 4{m_e}^2\gamma^\nu \\
= \;& 2(\not l+\not Q-m_e)\gamma^\mu(\not l+\not P-m_e) + 2m_e\gamma^\mu(\not l+\not P-m_e) \\
& +2m_e(\not l+\not Q-m_e)\gamma^\mu + 4\gamma^\mu(l+P)(l+Q) - 4(l+P)^\mu(\not l+\not Q-m_e) \\
& -4(l+Q)^\mu(\not l+\not P-m_e) \\
= \;& 4\gamma^\mu(l+P)(l+Q) + 4m_e l^\mu - 4\not l(2l+P+Q)^\mu - 2\gamma^\mu l^2 \\
& +4l^\mu(\not l+\not Q-m_e) - 2(\not Q-m_e)\not l\gamma^\mu + 2\not l\gamma^\mu(\not P-m_e) \\
& +2(\not Q-m_e)\gamma^\mu(\not P-m_e) + 2m_e\gamma^\mu(\not P-m_e) + 2m_e(\not Q-m_e)\gamma^\mu \\
& -4(l+P)^\mu(\not Q-m_e) - 4(l+Q)^\mu(\not P-m_e) \\
= \;& 4\gamma^\mu(PQ + l(P+Q) + \frac{l^2}{2}) - 4\not l(P+Q+l)^\mu + 4m_e l^\mu \\
& +(\not Q-m_e)(2m_e\gamma^\mu - 2\not l\gamma^\mu - 4(l+P)^\mu + 4l^\mu) \\
& +(2m_e\gamma^\mu + 2\not l\gamma^\mu - 4(l+Q)^\mu)(\not P-m_e) \\
& +2(\not Q-m_e)\gamma^\mu(\not P-m_e) \\
= \;& 4\gamma^\mu(PQ + l(P+Q) + \frac{l^2}{2}) - 4\not l(P+Q+l)^\mu + 4m_e l^\mu \\
& +(\not Q-m_e)(2m_e\gamma^\mu + 2\gamma^\mu\not l - 4(l+P)^\mu) \\
& +(2m_e\gamma^\mu + 2\not l\gamma^\mu - 4(l+Q)^\mu)(\not P-m_e) \\
& +2(\not Q-m_e)\gamma^\mu(\not P-m_e) \qquad (3.21)
\end{aligned}$$

The first line of Eq. 3.21 contributes regardless of whether the fermion lines are on- or off-shell and can be found in standard textbooks, for example in Ref. [19]. In case one fermion line is on- the other one off-shell, either the second or third line, respectively, contributes in addition. The last term in Eq. 3.21 is only needed for the case where both P and Q are off-shell and thus will not enter into the present $\mathcal{O}(\alpha^2)$ level calculation. The mass-terms are retained only until the last stage of the FORM-reduction, after which only terms of $\mathcal{O}({m_e}^0)$ are kept; see the *ffac*-routines in Ref. [24] for details.
For initial state electron-line radiation, Eqs. 3.4, 3.12, the renormalized vertex function Γ^μ can be written as

$$\Gamma^\mu = FF\gamma^\mu + FF_a(\not{P}-\not{K})(P-K)^\mu + FF_b(\not{P}-\not{K})Q^\mu \tag{3.22}$$

With the previously defined notation for scalar integrals in section 3.1.1 for the external emission graphs A_1 and A_9, the decomposition 3.22 is done by the FORM-routine *ffac*, Ref. [24], and yields the following results for the various form-factor terms up to $\mathcal{O}({m_e}^0)$:

$$\begin{aligned} FF &= -2 - 4{m_e}^2 C_{1230} - 2t'C^\alpha_{123} + B^0_{23} + 2B^\alpha_{12} - 3B_{23} \\ &\quad -\frac{3\alpha}{t'+\alpha}(B^\alpha_{12} - B_{23}) \qquad (3.23) \\ FF_a &= \frac{2}{t'+\alpha}(B^\alpha_{12} - B_{23}) \qquad (3.24) \\ FF_b &= -4C^\alpha_{123} + \frac{4}{t'+\alpha}(B^0_{23} + \frac{3}{2} + \alpha C^\alpha_{123}) \\ &\quad + \frac{4}{(t'+\alpha)^2}(t'B^\alpha_{12} - \frac{3}{2}\alpha B^\alpha_{12} + \frac{1}{2}\alpha B_{23} - 2t'B_{23})\,, \qquad (3.25) \end{aligned}$$

for the off-shell graph A_1 and

$$\begin{aligned} FF^0 &= 2 - 4{m_e}^2 C_{1230} - 2t'C^0_{123} + 3B^0_{23} - 3B_{23} \qquad (3.26) \\ FF^0_a &= 0 \qquad (3.27) \\ FF^0_b &= 0\,, \qquad (3.28) \end{aligned}$$

for the on-shell graph A_9.
The identity $(\not{P}-\not{K})\gamma^\mu(\not{P}-\not{K}) = \alpha\gamma^\mu + 2(\not{P}-\not{K})(P-K)^\mu$ was used in the above decomposition as well as the renormalization condition that Γ^μ vanish on-shell and for zero transfer, $t' = 0$. Due to the choice of the polarization-vector ε^μ the expression $\langle Q,\lambda|\not{\varepsilon}|P,\lambda\rangle = 0$, which means that the form-factors FF_a and FF_b don't contribute to the aspired level of accuracy for $A_1(A_2)$ and $A_9(A_{10})$. They will, however, prove to be very useful for testing the internal consistency of the calculation, as will be discussed in chapter 6.2 and do contribute to the amplitudes 3.10, 3.11. While it is not directly apparent, it can easily be checked that all renormalized form factors are indeed finite and scale independent. Ref. [24] also demonstrates that the renormalization condition is met correctly.

Inserting Eq. 3.20 into the expression for A_1, Eq. 3.4, and using the decomposition Eq. 3.22 as well as the "magic" properties of ε_μ yields:

$$\begin{aligned}
A_1 &= \frac{ie^5}{16\pi^2}\langle Q',\lambda'|\,\gamma_\mu\,|P',\lambda'\rangle G_{\lambda,\lambda'}(t')\times \\
&\quad \langle Q,\lambda|\,\Gamma^\mu((P'-Q')^2,(P-K)^2,{m_e}^2)\,\frac{\not P-\not K}{-2PK}\,\not\varepsilon\,|P,\lambda\rangle \\
&= \frac{ie^5}{16\pi^2}\langle Q',\lambda'|\,\gamma_\mu\,|P',\lambda'\rangle G_{\lambda,\lambda'}(t')\times \\
&\quad \{\langle Q,\lambda|\gamma^\mu\,\frac{\not P-\not K}{-2PK}\,\not\varepsilon\,|P,\lambda\rangle\,FF \\
&\quad +\langle Q,\lambda|(\not P-\not K)^2\,\not\varepsilon\,|P,\lambda\rangle\,(FF_a(P-K)^\mu+FF_bQ^\mu)\,\} \\
&= \frac{ie^5}{16\pi^2}\langle Q',\lambda'|\,\gamma_\mu\,|P',\lambda'\rangle G_{\lambda,\lambda'}(t')\times \\
&\quad \langle Q,\lambda|\gamma^\mu\,\frac{\not P-\not K}{-2PK}\,\not\varepsilon\,|P,\lambda\rangle\,FF \\
&= \frac{e^2}{16\pi^2}\,A_{e^-}^{TL}\,FF((P'-Q')^2,(P-K)^2)\,\delta_{\rho,-\lambda}
\end{aligned} \tag{3.29}$$

For A_2 one gets analogously:

$$A_2 = \frac{e^2}{16\pi^2}\,A_{e^-}^{TL}\,FF((P'-Q')^2,(Q+K)^2)\,\delta_{\rho,\lambda} \tag{3.30}$$

Since the tree-level amplitude $A_{e^-}^{TL}$ already contains the helicity dependence implicitly it is convenient to write:

$$A_1+A_2 = \frac{e^2}{16\pi^2}\,A_{e^-}^{TL}\,FF(t',\gamma)\,, \tag{3.31}$$

with

$$\gamma = \begin{cases} {m_e}^2+2QK & ,\rho=\lambda \\ {m_e}^2-2PK & ,\rho=-\lambda \end{cases} \tag{3.32}$$

For the on-shell form-factor amplitudes A_9 and A_{10} the derivation is even more straightforward and gives:

$$A_9+A_{10} = \frac{e^2}{16\pi^2}\,A_{e^-}^{TL}\,FF^0(t') \tag{3.33}$$

As can be seen from the definition of the scalar integrals for the various form-factors the relation between FF and FF^0 is given by:

$$FF^0(t') = FF(t',\gamma={m_e}^2) \tag{3.34}$$

This correspondence is shown to hold numerically in Fig. 3.2.

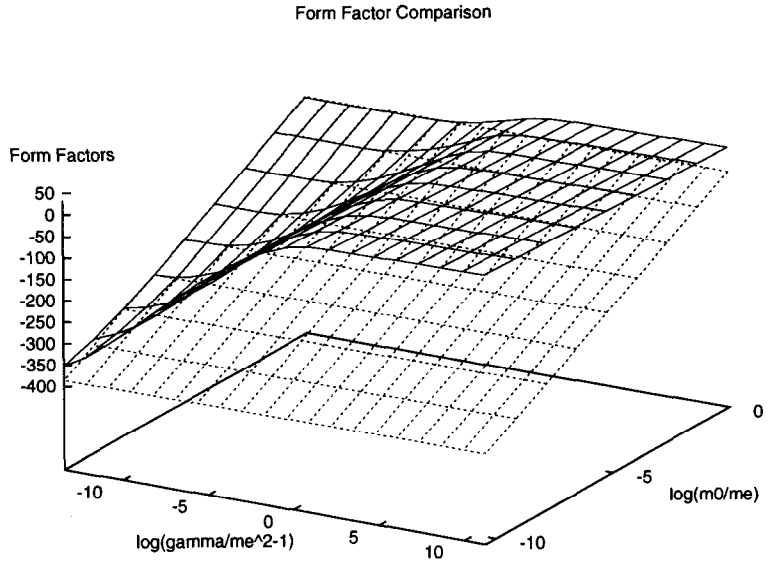

Figure 3.2: The real parts of the on-shell (dashed lines) and off-shell form factors for various values of $\frac{\gamma}{m_e{}^2} - 1$ at $t' = -1$. The off shell form factor is seen to approach FF^0 for $\gamma - m_e{}^2 \longrightarrow 0$, Eq. 3.32, and to have no $log\frac{m_0}{m_e}$ divergence for $\gamma \gg m_e{}^2$.

3.1.3 The Self-Energy Emission Amplitudes

The contribution from the off-shell self-energy emission amplitudes 3.10, 3.11 can be described by the expressions for the off-shell form factors 3.23, 3.24 and 3.25 in the limit of zero transfer ($t' = 0$) as follows:

$$\begin{aligned} \varepsilon_\mu \Gamma^\mu(K^2, P^2, (P-K)^2) &= FF \not{\varepsilon} + \varepsilon_\mu P^\mu (FF_a + FF_b)(\not{P} - \not{K}) \\ &= (-2 - 4m_e{}^2 C_{1230} + B^0_{23} - B^\alpha_{12}) \not{\varepsilon} + \\ &\quad \frac{\varepsilon_\mu P^\mu}{\alpha}(6 + 4B^0_{23} - 4B^\alpha_{12})(\not{P} - \not{K}) \end{aligned} \quad (3.35)$$

Using the above limit and decomposition gives for amplitude 3.10:

$$\begin{aligned} A_7 &= \frac{e^2}{16\pi^2}(-2 - 4m_e{}^2 C_{1230} + B^0_{23} - B^\alpha_{12}) A^{TL}_{e^-} + \\ &\quad \frac{ie^5}{16\pi^2}(6 + 4B^0_{23} - 4B^\alpha_{12})\frac{\varepsilon_\mu P^\mu}{\alpha} G_{\lambda,\lambda'}(t') \langle Q', \lambda' | \gamma_\mu | P', \lambda' \rangle \langle Q, \lambda | \gamma^\mu | P, \lambda \rangle \end{aligned}$$

$$
\begin{aligned}
&= \frac{e^2}{16\pi^2}\left(-2-4{m_e}^2 C_{1230}+B^0_{23}-B^\alpha_{12}\right)A^{TL}_{e^-} + \\
&\quad \frac{ie^5}{16\pi^2\alpha}\left(6+4B^0_{23}-4B^\alpha_{12}\right)\left[\frac{2\varepsilon_\mu P^\mu \delta_{\lambda,-\rho}}{t+\beta}G_{\lambda,\lambda'}(t')\ \times\right. \\
&\quad \left.\langle Q',\lambda'|\not{Q}\,|P',\lambda'\rangle\,\langle Q,\lambda|\not{K}\,|P,\lambda\rangle\ -\ \frac{\alpha t A^{TL}_{e^-}}{2ie^3(t+\beta)}\right] \\
&= \frac{e^2}{16\pi^2}\left(\frac{t-\beta}{t+\beta}\left[B^\alpha_{12}-B^0_{23}\right]-4{m_e}^2 C_{1230}-\frac{5t+2\beta}{t+\beta}\right)A^{TL}_{e^-} + \\
&\quad \frac{ie^5}{16\pi^2}\frac{2\varepsilon_\mu P^\mu}{(t+\beta)}\frac{\delta_{\lambda,-\rho}}{\alpha}\left(6+4B^0_{23}-4B^\alpha_{12}\right)G_{\lambda,\lambda'}(t')\ \times \\
&\quad \langle Q',\lambda'|\not{Q}\,|P',\lambda'\rangle\,\langle Q,\lambda|\not{K}\,|P,\lambda\rangle
\end{aligned}
\tag{3.36}
$$

The important identity 2.40 was used in deriving the result in 3.36, in which all terms proportional to $A^{TL}_{e^-}$ were identified. As will be discussed in more detail in chapter 7.3, terms multiplying the $\mathcal{O}(\alpha)$ single bremsstrahlung tree level amplitude contain the biggest corrections to the $\mathcal{O}(\alpha^2)$ cross section. The result for A_8 can be obtained from Eq. 3.36 through the crossing rule 2.22:

$$A_8 \;=\; A_7(P \leftrightarrow -Q, \lambda \rightarrow -\lambda) \tag{3.37}$$

3.2 The Electron Self-Energy Function

The contribution of the amplitudes given by Eqs. 3.8, 3.9 are determined by the solution of the electron self-energy function

$$\Sigma_o(P,m_0,m_e) \;=\; \frac{1}{i\pi^2}\int \mu^\epsilon d^n l \frac{\gamma_\nu(\not{P}+\not{l}+m_e)\gamma^\nu}{(l^2-{m_0}^2)((P+l)^2-{m_e}^2)+i\epsilon} \tag{3.38}$$

$$\equiv\; \Sigma^a_o(P^2,m_0,m_e)\,m_e \;+\; \Sigma^b_o(P^2,m_0,m_e)\not{P} \tag{3.39}$$

The proper treatment of the mass terms in the expression 3.38 for the self-energy contribution is essential here, since there are two independent renormalization constants in $\Sigma_o(P,m_0,m_e)$. In keeping with the hitherto adopted on-shell renormalization scheme, these two constants are fixed by imposing the renormalization conditions

$$\Sigma(P,m_0,m_e)\Big|_{\not{P}=m_e} \;=\; 0 \tag{3.40}$$

$$\left.\frac{\partial\Sigma(P,m_0,m_e)}{\partial P_\mu}\right|_{\not{P}=m_e} \;=\; 0 \tag{3.41}$$

The renormalization condition 3.41 is the reason why the terms proportional to m_e matter here: $\frac{\partial\Sigma^a}{\partial P_\mu}\Big|_{\not{P}=m_e}$ contains terms proportional to $\frac{1}{m_e}$. After prop-

erly taking these into account, the FORM-routine selfen, Ref. [24], gives the following result:

$$\begin{aligned}\Sigma(P,m_0,m_e) &= \left[4\left(B_{12}^{\alpha}-B_{12}^{0}\right)-4m_e{}^2C_{1230}-2\right]m_e + \\ &\quad \left[4m_e{}^2C_{1230}-\left(B_{12}^{\alpha}-B_{12}^{0}\right)\left(1+\frac{m_e{}^2}{P^2}\right)-\frac{m_e{}^2}{P^2}+3\right]\not{P} \\ &\approx \left[4m_e{}^2C_{1230}-\left(B_{12}^{\alpha}-B_{12}^{0}\right)+3\right]\not{P} \qquad (3.42)\end{aligned}$$

The mass-terms can be dropped in the final step in Eq. 3.42 since it represents the renormalized result. Doing the same at an earlier stage, however, would give the wrong $\Sigma^b(P^2,m_0,m_e)$-function. Eq. 3.42 is also clearly finite and scale independent. The "C_0" function enters the self-energy result, a term with only two propagators, through the derivative in 3.41 and is given explicitly in Eq. 3.19. Inserting this result into Eq. 3.8 yields:

$$\begin{aligned}A_5 &= \frac{ie^5}{16\pi^2}\langle Q',\lambda'|\,\gamma_\mu|P',\lambda'\rangle G_{\lambda,\lambda'}(t')\times \\ &\quad \langle Q,\lambda|\,\gamma^\mu\frac{\not{P}-\not{K}}{-2PK}\,\Sigma^b((P-K)^2,m_0,m_e)(\not{P}-\not{K})\,\frac{\not{P}-\not{K}}{-2PK}\not{\epsilon}\,|P,\lambda\rangle \\ &= \frac{ie^5}{16\pi^2}\,\Sigma^b((P-K)^2,m_0,m_e)\,\langle Q',\lambda'|\,\gamma_\mu|P',\lambda'\rangle G_{\lambda,\lambda'}(t')\times \\ &\quad \langle Q,\lambda|\,\gamma^\mu\frac{\not{P}-\not{K}}{-2PK}\not{\epsilon}\,|P,\lambda\rangle \\ &= \frac{e^2}{16\pi^2}\,\Sigma^b((P-K)^2,m_0,m_e)\,A_{e^-}^{TL} \qquad (3.43)\end{aligned}$$

With the notation of Eq. 3.32 one finally gets:

$$A_5+A_6=\frac{e^2}{16\pi^2}\,\Sigma^b(\gamma,m_0,m_e)\,A_{e^-}^{TL} \qquad (3.44)$$

It is interesting to observe, that the IR-divergences contained in Eq. 3.44 are exactly canceled by the $ln\frac{m_0}{m_e}$ terms present in the expression for the amplitudes A_7 and A_8 in Eqs. 3.36 and 3.37. This set of graphs is also separately gauge invariant.

Standard Feynman techniques give 18 one photon exchange diagrams for the process considered here (modulo vacuum polarization) as was mentioned in section 3. From Eqs. 3.40, 3.41 it can readily be seen that all graphs with self-energy loops next to external lines don't contribute to the $\mathcal{O}(\alpha^2)$ calculation in the chosen on-shell renormalization scheme, since

$$\frac{\Sigma(P,m_0,m_e)}{\not{P}-m_e}\ \overset{\not{P}=m_e}{\longrightarrow}\ \frac{\partial\Sigma(P,m_0,m_e)}{\partial\not{P}}\ \overset{\not{P}=m_e}{\longrightarrow}\ 0 \qquad (3.45)$$

Thus

$$A_{11} = 0 \ , \ \ldots \ , \ A_{18} = 0 \tag{3.46}$$

This completes the $\mathcal{O}({m_e}^0)$ contributions of the $\mathcal{O}(\alpha^2)$ single bremsstrahlung amplitudes with real hard photon emission off external legs. The next section will now deal with the much more complicated situation given for internal photon emission in amplitudes Eqs. 3.6, 3.7.

3.3 The Internal Emission Amplitudes

3.3.1 Scalar Integrals

The FORM notation of scalar integrals used in the decomposition of the tensor integrals 3.6, 3.7 differs from the notation used in previous sections for the obvious reason that there are now four propagators inside the loop. This leads to the following identifications:

$$\begin{aligned}
B_{12} &= B_0({m_e}^2; m_0, m_e) && (3.47)\\
B^{\alpha}_{13} &= B_0({m_e}^2 - \alpha; m_0, m_e) && (3.48)\\
B_{24} &= B_0(2{m_e}^2 + t; m_e, m_e) && (3.49)\\
B_{34} &= B_0(2{m_e}^2 + t'; m_e, m_e) && (3.50)\\
C^{\alpha}_{123} &= C_0({m_e}^2, {m_0}^2, {m_e}^2 - \alpha; m_0, m_e, m_e) && (3.51)\\
C_{124} &= C_0({m_e}^2, 2{m_e}^2 + t, {m_e}^2; m_0, m_e, m_e) && (3.52)\\
C^{\alpha}_{134} &= C_0({m_e}^2 - \alpha, 2{m_e}^2 + t', {m_e}^2; m_0, m_e, m_e) && (3.53)\\
C_{234} &= C_0({m_0}^2, 2{m_e}^2 + t', 2{m_e}^2 + t; m_e, m_e, m_e) && (3.54)\\
D^{\alpha}_{1234} &= D_0(m_e^2, m_0^2, 2m_e^2 + t', m_e^2, m_e^2 - \alpha, 2m_e^2 + t; m_0, m_e, m_e, m_e) , && (3.55)
\end{aligned}$$

where the basic B_0, C_0 and D_0 functions are defined in section 2.1 as usual.

3.3.2 The $A_3 + A_4$ Calculation

The numerator of Eq. 3.6 was put into the FORM-file $a3a4$ in which the outgoing term 3.7 was added through the crossing relation 2.22. By means of algebraic manipulations, the initial output of roughly 20000 (!) terms could be reduced to 90, which involved many rather complicated transformations (see appendices of Ref. [24]). Again, the identity 2.23 was crucial to achieve this step down to so relatively few terms as well as separating out the part proportional to A_e^{TL}. The result given by $a3a4$ reads

$$A_3 + A_4 = \frac{ie^5}{16\pi^2} G_{\lambda,\lambda'}(t') \left(F_0 \mathcal{I}_0 + F_1 \mathcal{I}_1 + F_2 \mathcal{I}_2 \right) \ , \tag{3.56}$$

where

$$\mathcal{I}_0 = 2\sqrt{2}\rho \langle P', Q' \rangle_{-\rho} \frac{(\langle h, h' \rangle_\rho)^2}{\langle P, K \rangle_\rho \langle Q, K \rangle_\rho} \tag{3.57}$$

$$\mathcal{I}_1 = 2\sqrt{2}\lambda \frac{\langle \widehat{h}, K\rangle_{-\rho}}{\langle \widehat{h}, K\rangle_{\rho}} \frac{\langle Q', \lambda' | \not{K} | P', \lambda'\rangle}{\langle P, Q\rangle_{-\rho}} \tag{3.58}$$

$$\mathcal{I}_2 = 2\sqrt{2}\lambda \frac{\langle \widehat{h}, K\rangle_{-\rho}}{\langle \widehat{h}, K\rangle_{\rho}} \frac{\langle Q', \lambda' | \not{\widehat{K}} | P', \lambda'\rangle}{\langle P, Q\rangle_{-\rho}} \tag{3.59}$$

The function $\mathcal{I}_0$ is proportional to the electron-line tree level amplitude:

$$A_{e^-}^{TL} = ie^3 G_{\lambda,\lambda'}(t')\, \mathcal{I}_0 \tag{3.60}$$

The form factors are

$$\begin{aligned} F_0(\rho=\lambda) = & -2(tC_{124} - t'C_{134}^{-\beta}) - (B_{13}^{-\beta} - B_{34})3\beta(t-\alpha)^{-1} \\ & - \{tC_{124} - \alpha C_{123}^{\alpha} - (t+\beta)C_{134}^{\alpha} + (\alpha-\beta)C_{234} + \alpha t D_{1234}^{\alpha}\} \\ & \qquad \times t\beta^{-1}(\alpha-\beta)(t-\alpha)^{-1} \\ & + \{tC_{124} + \beta C_{123}^{-\beta} - (t-\alpha)C_{134}^{-\beta} + (\alpha-\beta)C_{234} - \beta t D_{1234}^{-\beta}\} \\ & + (B_{13}^{\alpha} - B_{34})\,\alpha(t-\alpha)^{-1}\{1 - 3t(t+\beta)^{-1}\} \\ & + (B_{24} - B_{34})\,2t\alpha(\alpha-\beta)^{-1}(t-\alpha)^{-1} + (B_{12} - B_{13}^{-\beta})2t(t-\alpha)^{-1} \end{aligned} \tag{3.61}$$

$$\begin{aligned} F_1(\rho=\lambda) = & \; 2t(\alpha-\beta)^{-1} \\ & + \{tC_{124} - \alpha C_{123}^{\alpha} - (t+\beta)C_{134}^{\alpha} + (\alpha-\beta)C_{234} + \alpha t D_{1234}^{\alpha}\} \\ & \qquad \times\{tt'\beta^{-2}(t-\alpha)^{-1}(t-\beta) + \tfrac{1}{2}\delta_{\rho,1}\} \\ & - \{tC_{124} + \beta C_{123}^{-\beta} - (t-\alpha)C_{134}^{-\beta} + (\alpha-\beta)C_{234} - \beta t D_{1234}^{-\beta}\} \\ & \qquad \times\{\tfrac{1}{2}\alpha^{-1}\beta\delta_{\rho,-1}\} \\ & + (B_{13}^{-\beta} - B_{12})\,2t(t-\alpha)^{-1} \\ & + (B_{13}^{\alpha} - B_{34})\,tt'(t-\alpha)^{-1}\{2\beta^{-1} - 3(t+\beta)^{-1}\} \\ & + 2(B_{24} - B_{34})\,tt'(\alpha-\beta)^{-1}\{(\alpha-\beta)^{-1} - t\beta^{-1}(t-\alpha)^{-1}\} \end{aligned} \tag{3.62}$$

$$\begin{aligned} F_2(\rho=\lambda) = & -2t(\alpha-\beta)^{-1} + t(t+\beta)^{-1} \\ & - \{tC_{124} - \alpha C_{123}^{\alpha} - (t+\beta)C_{134}^{\alpha} + (\alpha-\beta)C_{234} + \alpha t D_{1234}^{\alpha}\} \\ & \qquad \times\{tt'\beta^{-2} + \tfrac{1}{2}\alpha\beta^{-1}\delta_{\rho,1}\} \\ & + \{tC_{124} + \beta C_{123}^{-\beta} - (t-\alpha)C_{134}^{-\beta} + (\alpha-\beta)C_{234} - \beta t D_{1234}^{-\beta}\} \\ & \qquad \times\{\tfrac{1}{2}\delta_{\rho,-1}\} \\ & + (B_{34} - B_{13}^{\alpha})\,tt'(t+\beta)^{-1}\{2\beta^{-1} + (t+\beta)^{-1}\} \\ & + 2(B_{24} - B_{34})\,tt'(\alpha-\beta)^{-1}\{\beta^{-1} - (\alpha-\beta)^{-1}\} \end{aligned} \tag{3.63}$$

The opposite helicity cases may be obtained from the above results using the substitutions (for $i = 0, 1, 2$):

$$F_i(\rho = -\lambda, \alpha, \beta) = F_i(\rho = \lambda, -\beta, -\alpha) \tag{3.64}$$

While Eq. 3.56 still does not look very transparent, several observations may help to clarify the overall picture. Since the amplitudes 3.6 and 3.7 are not UV-divergent one should evidently expect this feature for the result 3.56, where all B_0 terms possess such an infinite contribution (see section 2.1). A simple check in the FORM routine *a3a4*, which replaced each B_{ij} by $B_{ij} + div$, proved that all divergences cancel properly. This procedure also insures the scale independence of Eq. 3.56. Numerical analysis revealed that in the case of amplitude A_3, for instance, only C_{124} and D^{α}_{1234}have IR-divergent terms, regulated by the virtual photon mass m_0. By closer examining the four denominators in 3.6, it becomes clear that , except for $K^0 = 0$, only propagators 1, 2 & 4 taken together and with no loop momentum left in the numerator can lead to a logarithmic divergence in m_0, confirming the numerical findings. From Ref. [31] and for $\frac{m_e^2}{-t} \ll 1$ one has:

$$C_{124} = \frac{1}{t}\left[\frac{1}{2} ln^2 \frac{m_e^2}{-t} + ln\frac{m_e^2}{-t} ln\frac{m_0^2}{m_e^2} - \frac{\pi^2}{6}\right], \tag{3.65}$$

and for $m_0 \to 0$:

$$D^{\alpha}_{1234} \sim -\frac{1}{\alpha t} ln\frac{m_e^2}{-t} ln\frac{m_0^2}{m_e^2} \tag{3.66}$$

Eqs. 3.65 and 3.66 corroborate that the only effective IR-divergent term in 3.56 is $-2tC_{124}\frac{ie^5}{16\pi^2}\mathcal{I}_0$, which coincides with the prediction of the IR-theory expounded on in chapter 5. It should also be noted that the form factors F_1 and F_2 are normalized in a slightly different way than the output printed in Ref. [24]. For comparison, the form factors here should be multiplied by $\frac{2}{t\beta}$ for $\rho = \lambda$. F_1 contains a contribution proportional to $(B_{13}^{-\beta} - B_{12})$ which will turn out to cancel the corresponding contribution from amplitude 3.36 and will thus make F_1 and F_2 almost symmetric in form. This feature will help concentrate the numerically relevant leading and subleading logarithmic terms in the part proportional to the tree level amplitude, as the results of this chapter will now be summarized in chapter 4.

Chapter 4

The Exact Differential $\mathcal{O}(\alpha^2)$ Result

In order to have a complete differential result it is necessary to express all amplitudes with the same notation of scalar integrals. Using the definitions of section 3.3.1 and the expressions given in Eqs. 3.31, 3.33, 3.36, 3.37 and 3.44 one gets the following for $\rho = -\lambda$:

$$\begin{aligned} & A_1 + A_2 + A_5 + A_6 + A_7 + A_8 + A_9 + A_{10} \\ = \; & \frac{e^2}{16\pi^2}\left\{-8 - \frac{\beta}{t+\beta} + B_{12}\frac{4t+6\beta}{t+\beta} + B_{13}^{\alpha}\frac{2t-3\alpha}{t'+\alpha} - \right. \\ & \left. B_{34}\frac{6t'+3\alpha}{t'+\alpha} - 8{m_e}^2 C_{123}^0 - 2t'C_{134}^{\alpha} - 2t'C_{134}^0\right\} A_{e^-}^{TL} \\ & - \frac{ie^5}{16\pi^2} G_{\lambda,\lambda'}(t')\left[2B_{13}^{\alpha} - 2B_{12} + 1\right]\frac{t}{t+\beta}\,\mathcal{I}_1\,, \end{aligned} \tag{4.1}$$

and thus for $\rho = \lambda$:

$$\begin{aligned} & A_1 + A_2 + A_5 + A_6 + A_7 + A_8 + A_9 + A_{10} \\ = \; & \frac{e^2}{16\pi^2}\left\{-8 + \frac{\alpha}{t-\alpha} + B_{12}\frac{4t-6\alpha}{t-\alpha} + B_{13}^{-\beta}\frac{2t+3\beta}{t'-\beta} - \right. \\ & \left. B_{34}\frac{6t'-3\beta}{t'-\beta} - 8{m_e}^2 C_{123}^0 - 2t'C_{134}^{-\beta} - 2t'C_{134}^0\right\} A_{e^-}^{TL} \\ & - \frac{ie^5}{16\pi^2} G_{\lambda,\lambda'}(t')\left[2B_{13}^{-\beta} - 2B_{12} + 1\right]\frac{t}{t-\alpha}\,\mathcal{I}_1 \end{aligned} \tag{4.2}$$

The exact $\mathcal{O}(\alpha^2)$ single bremsstrahlung result for electron-line emission and $\rho = \lambda$ is of course given by adding all amplitudes 3.4 + ... + 3.13 and with Eqs. 3.56 and 4.2 reads for $\rho = \lambda$:

$$A_{e^-} = \frac{ie^5}{16\pi^2} G_{\lambda,\lambda'}(t') \left(\mathcal{F}_0\mathcal{I}_0 + \mathcal{F}_1\mathcal{I}_1 + \mathcal{F}_2\mathcal{I}_2\right) , \tag{4.3}$$

where the notation of Eqs. 3.57, 3.58 and 3.59 has been used. The form factors are

$$\begin{aligned}
\mathcal{F}_0(\rho=\lambda) = & -8 + \alpha(t-\alpha)^{-1} - 8m_e{}^2 C^0_{123} - 2(tC_{124} + t'C^0_{134}) \\
& - \{tC_{124} - \alpha C^{\alpha}_{123} - (t+\beta)C^{\alpha}_{134} + (\alpha-\beta)C_{234} + \alpha t D^{\alpha}_{1234}\} \\
& \qquad \times t\beta^{-1}(\alpha-\beta)(t-\alpha)^{-1} \\
& + \{tC_{124} + \beta C^{-\beta}_{123} - (t-\alpha)C^{-\beta}_{134} + (\alpha-\beta)C_{234} - \beta t D^{-\beta}_{1234}\} \\
& + 6B_{12} + (B^{\alpha}_{13} - B_{34})\,\alpha(t-\alpha)^{-1}\{1 - 3t(t+\beta)^{-1}\} \\
& - 6B_{34} + (B_{24} - B_{34})\{2t\alpha(\alpha-\beta)^{-1}(t-\alpha)^{-1}\}
\end{aligned} \tag{4.4}$$

$$\begin{aligned}
\mathcal{F}_1(\rho=\lambda) = & \; 2t(\alpha-\beta)^{-1} - t(t-\alpha)^{-1} \\
& + \{tC_{124} - \alpha C^{\alpha}_{123} - (t+\beta)C^{\alpha}_{134} + (\alpha-\beta)C_{234} + \alpha t D^{\alpha}_{1234}\} \\
& \qquad \times\{tt'\beta^{-2}(t-\alpha)^{-1}(t-\beta) + \tfrac{1}{2}\delta_{\rho,1}\} \\
& - \{tC_{124} + \beta C^{-\beta}_{123} - (t-\alpha)C^{-\beta}_{134} + (\alpha-\beta)C_{234} - \beta t D^{-\beta}_{1234}\} \\
& \qquad \times\{\tfrac{1}{2}\alpha^{-1}\beta\delta_{\rho,-1}\} \\
& + (B^{\alpha}_{13} - B_{34})\,tt'(t-\alpha)^{-1}\{2\beta^{-1} - 3(t+\beta)^{-1}\} \\
& + 2(B_{24} - B_{34})\,tt'(\alpha-\beta)^{-1}\{(\alpha-\beta)^{-1} - t\beta^{-1}(t-\alpha)^{-1}\}
\end{aligned} \tag{4.5}$$

$$\begin{aligned}
\mathcal{F}_2(\rho=\lambda) = & -2t(\alpha-\beta)^{-1} + t(t+\beta)^{-1} \\
& - \{tC_{124} - \alpha C^{\alpha}_{123} - (t+\beta)C^{\alpha}_{134} + (\alpha-\beta)C_{234} + \alpha t D^{\alpha}_{1234}\} \\
& \qquad \times\{tt'\beta^{-2} + \tfrac{1}{2}\alpha\beta^{-1}\delta_{\rho,1}\} \\
& + \{tC_{124} + \beta C^{-\beta}_{123} - (t-\alpha)C^{-\beta}_{134} + (\alpha-\beta)C_{234} - \beta t D^{-\beta}_{1234}\} \\
& \qquad \times\{\tfrac{1}{2}\delta_{\rho,-1}\} \\
& + (B_{34} - B^{\alpha}_{13})\,tt'(t+\beta)^{-1}\{2\beta^{-1} + (t+\beta)^{-1}\} \\
& + 2(B_{24} - B_{34})\,tt'(\alpha-\beta)^{-1}\{\beta^{-1} - (\alpha-\beta)^{-1}\}
\end{aligned} \tag{4.6}$$

The opposite helicity cases may again be obtained from the above results using the substitutions (for $i = 0, 1, 2$):

$$\mathcal{F}_i(\rho=-\lambda,\alpha,\beta) = \mathcal{F}_i(\rho=\lambda,-\beta,-\alpha) \tag{4.7}$$

In Figs. 4.1 and 4.2 the differential result 4.3 is compared to a recent calculation by Fadin et al. [43] after the IR-divergent terms were properly removed (see chapter 5).

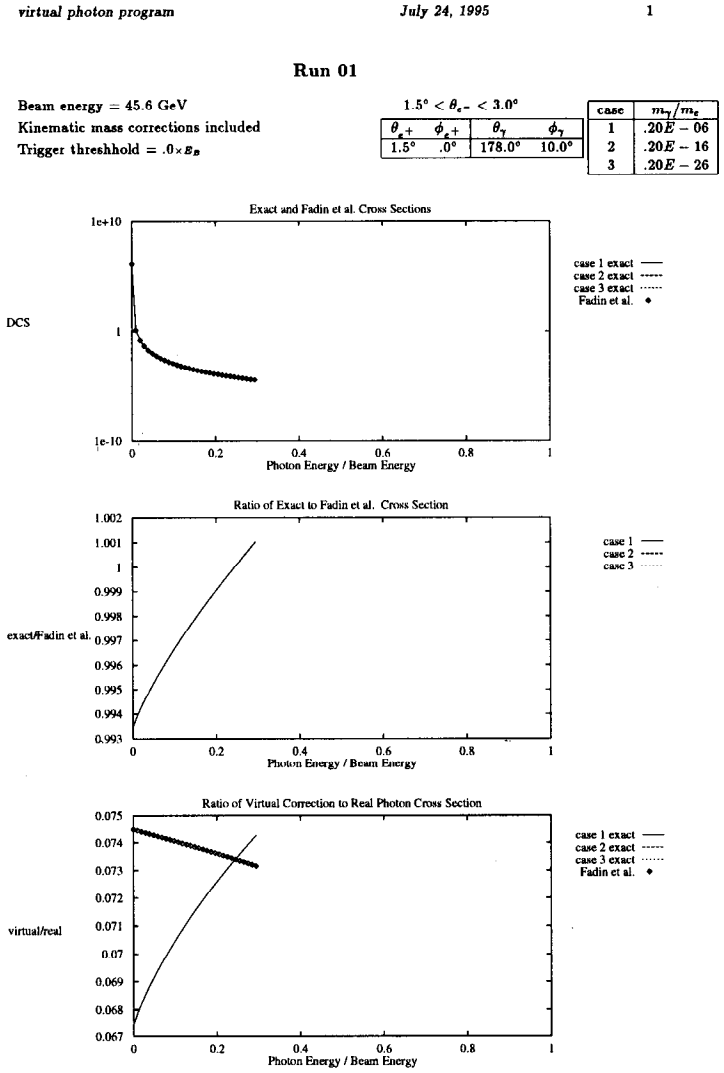

Figure 4.1: A comparison of the exact differential expression 4.3 to the result given by Fadin et al. [43]. The graph on top displays $|\mathcal{M}^{\mathcal{O}(\alpha+\alpha^2)}|^2 - 2\alpha[Re(B(t))+Re(B(t'))]|\mathcal{M}^{\mathcal{O}(\alpha)}|^2$ (see chapter 5), i.e. there is no IR-dependence (m_0 or E_{cut}) left over. $\mathcal{M}$ denotes the invariant matrix elements for the respective cases. The second figure shows the ratio of the two calculations explicitly over the range of available photon energies and the bottom graph gives the size of the $\mathcal{O}(\alpha^2)$ virtual corrections to the differential $\mathcal{O}(\alpha)$ single hard bremsstrahlung cross section.

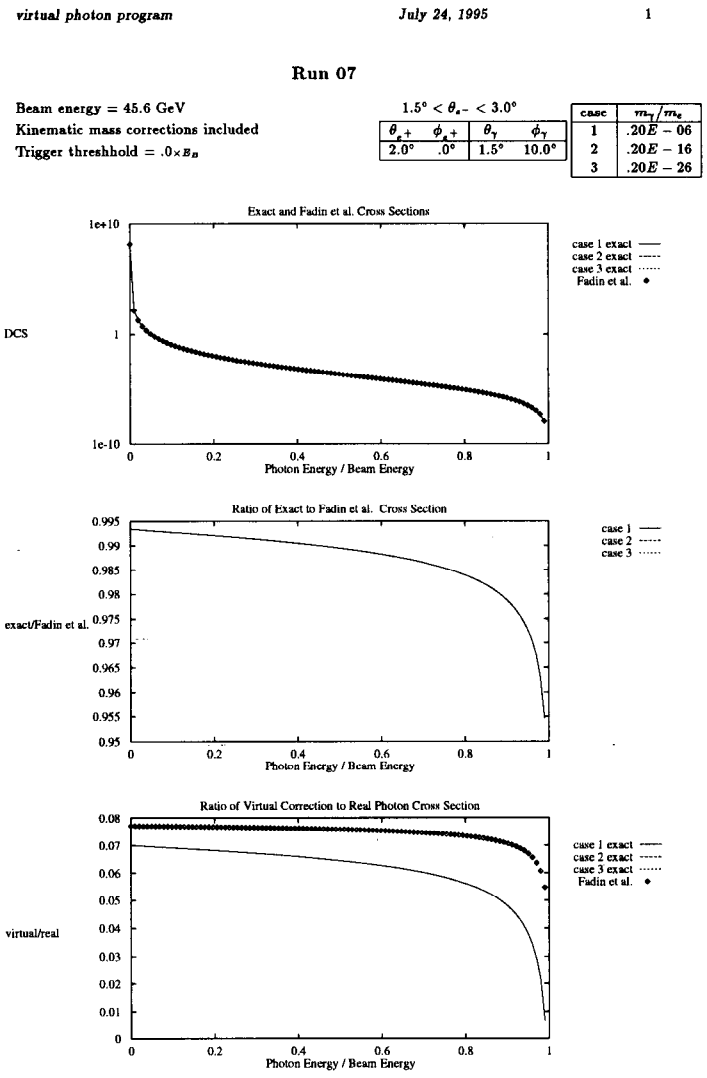

Figure 4.2: This figure is analogous to Fig 4.1 but shows the same comparison for a different set of photon and positron angles. While run1 has the bremsstrahlung photon close to the incoming electron direction, this graph has the emitted photon along the incoming positron line. Although the respective lines are dominating in each case, both figures are using the contribution from the complete two line t-channel expression.

The agreement between these two differential results is roughly within 5% over the range of available real photon energies. This should be compared to the overall size of the second order correction to the Born process, which is about $3.5pm$ [45]. The soft limit, however, disagrees, which will become more important for the integrated cross section since it is the regime with the highest emission probability [3]. As can also be seen in both figures, there is no virtual photon-mass dependence left. The one graph that is shown is actually three identical graphs for three different values of m_0 (compare with figure legend). The general treatment of the expected IR-behaviour is discussed in chapter 5 in the context of Yennie, Frautschi and Suura theory [4]. The expression is explicitly scale independent, as is expected of every physically meaningful result. This holds not only for 4.3 but also for all equations that have contributed to the final answer. It is also worth mentioning that the by far largest part of the answer 4.3 is concentrated in only 18 terms, namely those contained in $\mathcal{F}_0$. Numerical tests showed that on the scale of Figs. 4.1 and 4.2 no noticeable change could be observed. Since these represent only one dimensional cuts through a multidimensional phase space, this aspect needs to be revisited in the context of Monte Carlo (MC) phase space integration.
Eq. 4.3 is the central result of the presented work; it describes the fully differential $\mathcal{O}(\alpha^2)$ single bremsstrahlung corrections to low angle Bhabha scattering, which is essential for any MC-implementation [34]. It is thus of primary importance for the theoretical luminosity determination below the $1pm$ precision level. In order to convey a more in depth understanding about the validity of the presented work, part *II* of this thesis will mostly be devoted to demonstrate that Eq. 4.3 satisfies all theoretical expectations and is in good agreement with leading log calculations. Also Monte Carlo results for the fully integrated cross section will be presented for a SICAL-type acceptance [45, 36].

Part II

Consistency Checks & MC Results

Chapter 5

Yennie, Frautschi & Suura Theory

Although quantum field theories with massless gauge bosons display both short- (UV) and long-distance (IR) divergences in certain types of graphs, it has long been known that the nature of the two infinities have very different origins [23, 15]. While the UV-divergences are a manifestation of our ignorance about small-scale physics and cannot be avoided in theories that assume point-like elementary particles, the genuine infinite wavelength divergences should never be "real", i.e. should cancel out of the final result for any cross section. The cancelation of the first order IR-divergences in QED was first proven by Bloch and Nordsieck [9] as early as 1937. It took, however, almost another quarter of a century until the IR-problem was understood comprehensively to all orders in the fundamental work by Yennie, Frautschi and Suura (YFS) [4]. Since the YFS-theory gives a well defined IR-limit for the amplitude 3.56, it is necessary at this point to give a brief review of the IR-theory. α in this chapter denotes the fine-structure constant.

5.1 The YFS B & $\widetilde{B}$ Functions

Consider the expansion of the full connected amplitude for s-channel Bhabha scattering at $\sqrt{s} = M_Z$ in terms of the number of virtual photon loops. One can then write [4]

$$M(P,P') = \sum_{n=0}^{\infty} M_n(P,P') \,, \tag{5.1}$$

where $M_n(P,P')$ is the contribution of all n virtual γ-loop graphs to $M(P,P')$. The result obtained by Yennie, Frautschi and Suura is that

$$M_n(P,P') \;=\; \sum_{r=0}^{n} m_{n-r}(P,P')\frac{(\alpha B)^r}{r\,!}\;, \tag{5.2}$$

where the $m_j(P,P')$ do not have virtual IR-divergences and are of order α^j relative to $M_0 = m_0$. The virtual infrared function $B(s)$ is such that

$$\begin{aligned} B(s) \;&=\; \frac{i}{(2\pi)^3}\int \frac{d^4k}{k^2-m_0{}^2+i\epsilon}\left[\frac{-2P'_\mu-k_\mu}{-2P'k-k^2-i\epsilon}-\frac{2P_\mu-k_\mu}{2Pk-k^2-i\epsilon}\right]^2\;, \\ Re\;B(s) \;&=\; \frac{-1}{2\pi}\left[ln\frac{s}{m_e{}^2}\left(2ln\frac{m_e}{m_0}+\frac{1}{2}ln\frac{s}{m_e{}^2}-\frac{1}{2}\right)-2ln\frac{m_e}{m_0}+1-\frac{2\pi^2}{3}\right] \end{aligned} \tag{5.3}$$

Hence

$$M(P,P') \;=\; e^{\alpha B}\sum_{n=0}^{\infty} m_n(P,P') \tag{5.4}$$

This is the famous exponentiation of virtual infrared divergences of the YFS program. To complete the review of the YFS-theory, consider next the differential cross section for the process $e^+ + e^- \to n(\gamma) + X$, where $n(\gamma)$ represents the emission of n real photons with four-momenta $k_1, ..., k_n$. For a given value of n, this differential cross section is

$$d\sigma = e^{2\alpha Re\,B}\frac{1}{n\,!}\int\prod_{j=1}^{n}\frac{dE_X d^3k_j}{\sqrt{k_j{}^2+m_0{}^2}}\,\delta\left(\sqrt{s}-E_X-\sum_{i=1}^{n}k_i{}^0\right)\left[\sum_{l=0}^{\infty}m_l{}^{(n)}\right]^2\;, \tag{5.5}$$

where $m_l{}^{(n)}$ is a special case of m_j in 5.4 in which X involves n real photons. The second theorem of Yennie, Frautschi and Suura is that

$$\begin{aligned} \left[\sum_{l=0}^{\infty}m_l{}^{(n)}\right]^2 \;=\; &\widetilde{S}(k_1)...\widetilde{S}(k_n)\widetilde{\beta}_0+\sum_{i=1}^{n}\widetilde{S}(k_1)...\widetilde{S}(k_{i-1})\widetilde{S}(k_{i+1})...\widetilde{S}(k_n)\widetilde{\beta}_1(k_i)+... \\ &+\sum_{i=1}^{n}\widetilde{S}(k_i)\widetilde{\beta}_{n-1}(k_1,...,k_{i-1},k_{i+1},...,k_n)+\widetilde{\beta}_n(k_1,...,k_n)\;, \end{aligned} \tag{5.6}$$

where $\widetilde{\beta}_j$ is IR-divergence free and is of order α^j relative to $\widetilde{\beta}_0$. The real infrared divergence function $\widetilde{S}(k)$ is given by

$$\widetilde{S}(k) \;=\; -\frac{\alpha}{4\pi^2}\left[\frac{P_\mu}{kP}-\frac{P'_\mu}{kP'}\right]^2 \tag{5.7}$$

It follows that the cross section for the emission of an arbitrary number of real photons can be written as

$$d\sigma = e^{2\alpha(Re\,B+\widetilde{B})}\frac{1}{2\pi}\int_{-\infty}^{\infty}dy\,e^{iy(\sqrt{s}-E_X)+D} \times \left[\widetilde{\beta}_0+\sum_{n=1}^{\infty}\frac{1}{n!}\int\prod_{j=1}^{n}\frac{d^3k_j}{k_j^0}e^{-iyk_j^0}\widetilde{\beta}_n\right]dE_X\,, \tag{5.8}$$

with D and $\widetilde{B}$ defined as follows:

$$D = \int^{k^0\le E_{cut}}\frac{d^3k}{k^0}(e^{-iyk^0}-1)\widetilde{S}\,, \tag{5.9}$$

and

$$\begin{aligned}\widetilde{B}(s,E_{cut}) &= \int^{k^0\le E_{cut}}\frac{d^3k}{\sqrt{k^2+m_0^2}}\frac{\widetilde{S}(k)}{2\alpha}\\ &= \frac{1}{2\pi}\left[ln\frac{s}{m_e^2}\left(2ln\frac{m_e}{m_0}+\frac{1}{2}ln\frac{s}{m_e^2}-ln\frac{EE'}{E_{cut}^2}\right)\right.\\ &\qquad\left.-2ln\frac{m_e}{m_0}+ln\frac{EE'}{E_{cut}^2}-\frac{\pi^2}{3}\right]\end{aligned} \tag{5.10}$$

From the explicit forms in Eqs. 5.3 and 5.10 it can be verified that $Re\,B+\widetilde{B}$ is free of IR-divergences so that $d\sigma$ in 5.8 is indeed a physically meaningful quantity and exhibits the cancelation of infrared divergences to all orders in α. It should be mentioned that the infrared functions given above are expressed in the s-channel and that the t-channel expressions are derived from 5.3 and 5.10 with the analytical continuation technique and read [33]:

$$Re\;B(t) = \frac{-1}{2\pi}\left[ln\frac{-t}{m_e^2}\left(2ln\frac{m_e}{m_0}+\frac{1}{2}ln\frac{-t}{m_e^2}-\frac{1}{2}\right)-2ln\frac{m_e}{m_0}+1-\frac{\pi^2}{6}\right] \tag{5.11}$$

$$\begin{aligned}\widetilde{B}(t,E_{cut}) = \frac{1}{2\pi}&\left[ln\frac{-t}{m_e^2}\left(2ln\frac{m_e}{m_0}+\frac{1}{2}ln\frac{-t}{m_e^2}-ln\frac{E_PE_Q}{E_{cut}^2}\right)\right.\\ &\left.-2ln\frac{m_e}{m_0}+ln\frac{E_PE_Q}{E_{cut}^2}-\frac{\pi^2}{6}\right]\end{aligned} \tag{5.12}$$

It is with the real YFS-IR function 5.12 that the infrared limit of the internal emission result 3.56 was tested. Numerical results for two representative kinematical cases are shown in Figs. 5.1. As is explained in the figure captions, the result for the amplitudes A_1-A_{10} is shown to have the right IR-terms predicted by the YFS program.

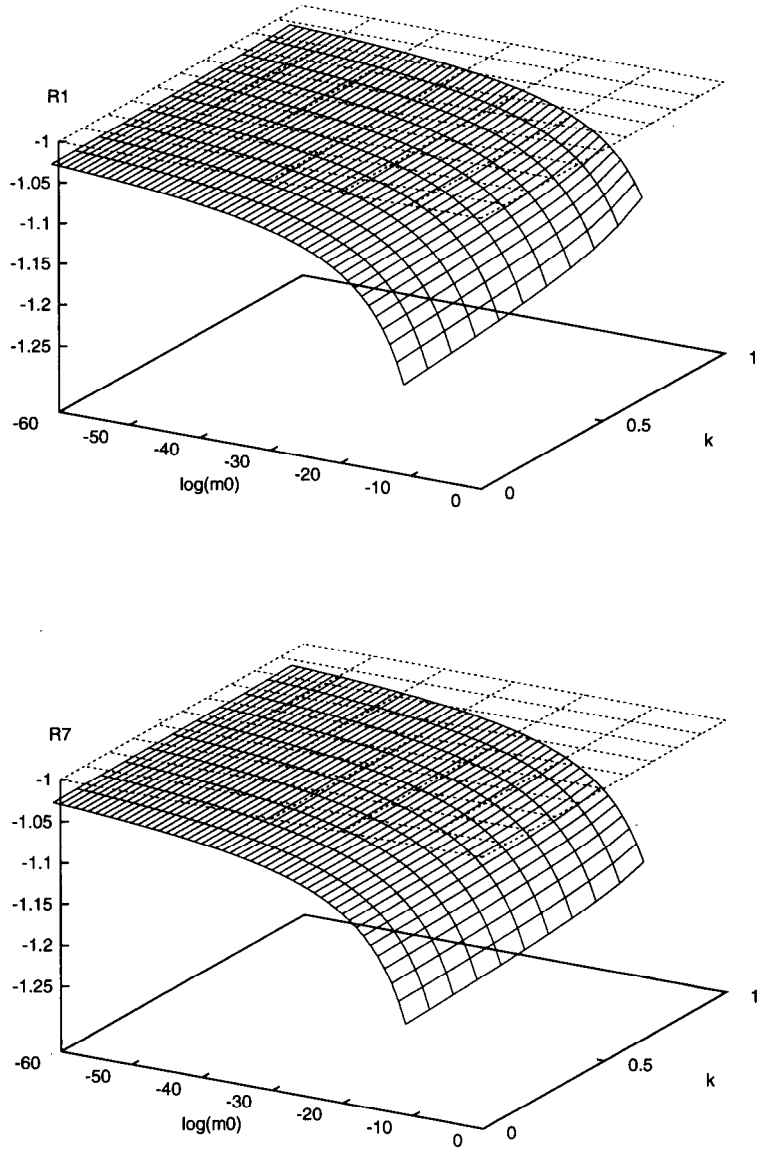

Figure 5.1: For the two separate runs, specified in Figs. 4.1, 4.2 as 1(R1) and 7(R7), the ratios of the squared invariant matrix elements resulting from the exact differential expression 4.3 versus $2\alpha(\widetilde{B}(t,E_{cut})+\widetilde{B}(t',E_{cut}))|\mathcal{M}^{\mathcal{O}(\alpha)}|^2$ are plotted. The limit $m_0 \longrightarrow 0$ should be $k = \frac{E_K}{E_{Beam}}$ independent and the ratios shown should approach -1 since the real YFS-functions are used. Both constraints are shown to hold for the result 4.3. The finite gap to -1 seen in both cases is of order $\frac{1}{log(m_0)}$.

Chapter 6

Gauge Variations

Ever since t'Hooft was able to prove the renormalizability of spontaneously broken gauge field theories [16], gauge invariance has become the dominant principle in modern particle physics. While it was long known that QED has gauge symmetry [2, 30], the weak and also the strong (QCD) nuclear force are now formulated through gauge invariance principles [23, 42]. Many of the consequences of gauge symmetries such as the Ward-Takahashi identities can be used as cross checks of results obtained from related amplitudes. One such cross check in the present calculation is a result of the gauge invariance of a subset of amplitudes and will be expounded on in the following sections.

6.1 Gauge Invariance

All physically observable quantities in the Standard Model must naturally be gauge invariant, however, also unobservable parts of those quantities can already display this symmetry. It can be shown that the amplitudes $\{A_1+A_2+A_3+A_4\}$, $\{A_5+A_6+A_7+A_8\}$ and $\{A_9+A_{10}\}$ are all separately gauge invariant. This will now be shown explicitly for the first bracket of amplitudes. Gauge invariance demands that longitudinal photons decouple from the amplitudes [30], thus by replacing $\not{\epsilon} \rightarrow \not{K}$ one gets:

$$A_1^{long} = \frac{e^5}{(2\pi)^4}\langle Q',\lambda'|\,\gamma_\mu\,|P',\lambda'\rangle G_{\lambda,\lambda'}(t')\times \int \frac{\mu^\epsilon d^n l}{-2PK}\frac{\langle Q,\lambda|\,\gamma_\nu(\not{l}+\not{Q})\gamma^\mu(\not{l}+\not{P}-\not{K})\gamma^\nu(\not{P}-\not{K})\not{K}\,|P,\lambda\rangle}{(l^2-m_0{}^2)((l+P-K)^2-m_e{}^2)((l+Q)^2-m_e{}^2)+i\epsilon} \tag{6.1}$$

$$A_2^{long} = \frac{e^5}{(2\pi)^4}\langle Q',\lambda'|\,\gamma_\mu\,|P',\lambda'\rangle G_{\lambda,\lambda'}(t')\times \int \frac{\mu^\epsilon d^n l}{2QK}\frac{\langle Q,\lambda|\not{K}\,(\not{Q}+\not{K})\gamma_\nu(\not{l}+\not{Q}+\not{K})\gamma^\mu(\not{l}+\not{P})\gamma^\nu\,|P,\lambda\rangle}{(l^2-m_0{}^2)((l+P)^2-m_e{}^2)((l+Q+K)^2-m_e{}^2)+i\epsilon} \tag{6.2}$$

$$A_3^{long} = \frac{e^5}{(2\pi)^4}\langle Q',\lambda'|\gamma_\mu|P',\lambda'\rangle G_{\lambda,\lambda'}(t')\times \int \frac{d^4l\langle Q,\lambda|\gamma_\nu(\not l+\not Q)\gamma^\mu(\not l+\not P-\not K)\not K(\not l+\not P)\gamma^\nu|P,\lambda\rangle}{(l^2-m_0{}^2)((l+P)^2-m_e{}^2)((l+P-K)^2-m_e{}^2)((l+Q)^2-m_e{}^2)+i\epsilon} \tag{6.3}$$

$$A_4^{long} = \frac{e^5}{(2\pi)^4}\langle Q',\lambda'|\gamma_\mu|P',\lambda'\rangle G_{\lambda,\lambda'}(t')\times \int \frac{d^4l\langle Q,\lambda|\gamma_\nu(\not l+\not Q)\not K(\not l+\not Q+\not K)\gamma^\mu(\not l+\not P)\gamma^\nu|P,\lambda\rangle}{(l^2-m_0{}^2)((l+P)^2-m_e{}^2)((l+Q+K)^2-m_e{}^2)((l+Q)^2-m_e{}^2)+i\epsilon} \tag{6.4}$$

Using the identities

$$(\not l+\not P-\not K)\not K(\not l+\not P) = (l+P)^2(\not l+\not P-\not K)-(l+P-K)^2(\not l+\not P) \tag{6.5}$$
$$(\not l+\not Q)\not K(\not l+\not Q+\not K) = -(l+Q)^2(\not l+\not Q+\not K)+(l+Q+K)^2(\not l+\not Q) \tag{6.6}$$

one gets

$$A_1^{long} = \frac{2e^5}{(2\pi)^4}\langle Q',\lambda'|\gamma_\mu|P',\lambda'\rangle G_{\lambda,\lambda'}(t')\times \int \mu^\epsilon d^nl\frac{\langle Q,\lambda|(\not l+\not P-\not K)\gamma^\mu(\not l+\not Q)|P,\lambda\rangle}{(l^2-m_0{}^2)((l+P-K)^2-m_e{}^2)((l+Q)^2-m_e{}^2)+i\epsilon} \tag{6.7}$$

$$A_2^{long} = -\frac{2e^5}{(2\pi)^4}\langle Q',\lambda'|\gamma_\mu|P',\lambda'\rangle G_{\lambda,\lambda'}(t')\times \int \mu^\epsilon d^nl\frac{\langle Q,\lambda|(\not l+\not P)\gamma^\mu(\not l+\not Q+\not K)|P,\lambda\rangle}{(l^2-m_0{}^2)((l+P)^2-m_e{}^2)((l+Q+K)^2-m_e{}^2)+i\epsilon} \tag{6.8}$$

$$A_3^{long} = -\frac{2e^5}{(2\pi)^4}\langle Q',\lambda'|\gamma_\mu|P',\lambda'\rangle G_{\lambda,\lambda'}(t')\times \left\{\int \mu^\epsilon d^nl\frac{\langle Q,\lambda|(\not l+\not P-\not K)\gamma^\mu(\not l+\not Q)|P,\lambda\rangle}{(l^2-m_0{}^2)((l+P-K)^2-m_e{}^2)((l+Q)^2-m_e{}^2)+i\epsilon} - \int \mu^\epsilon d^nl\frac{\langle Q,\lambda|(\not l+\not P)\gamma^\mu(\not l+\not Q)|P,\lambda\rangle}{(l^2-m_0{}^2)((l+P)^2-m_e{}^2)((l+Q)^2-m_e{}^2)+i\epsilon}\right\} \tag{6.9}$$

$$A_4^{long} = -\frac{2e^5}{(2\pi)^4}\langle Q',\lambda'|\gamma_\mu|P',\lambda'\rangle G_{\lambda,\lambda'}(t')\times$$

$$\Big\{ \int \mu^{\epsilon} d^n l \frac{\langle Q,\lambda|\,(\not{l}+\not{P})\gamma^{\mu}(\not{l}+\not{Q})\,|P,\lambda\rangle}{(l^2-{m_0}^2)((l+P)^2-{m_e}^2)((l+Q)^2-{m_e}^2)+i\epsilon}$$
$$- \int \mu^{\epsilon} d^n l \frac{\langle Q,\lambda|\,(\not{l}+\not{P})\gamma^{\mu}(\not{l}+\not{Q}+\not{K})\,|P,\lambda\rangle}{(l^2-{m_0}^2)((l+P)^2-{m_e}^2)((l+Q+K)^2-{m_e}^2)+i\epsilon} \Big\} \tag{6.10}$$

Thus it can readily be seen that

$$A_1^{long} + A_2^{long} + A_3^{long} + A_4^{long} \;=\; 0\,, \tag{6.11}$$

which proves that $\{A_1 + A_2 + A_3 + A_4\}$ is gauge invariant. The proof for the other sums of amplitudes mentioned above proceeds analogously.

6.2 The Internal Emission Gauge Variation

It follows from the definition of the vertex function 3.20 and the decomposition 3.22 that

$$\begin{aligned}
A_3^{long} \;=\;& \frac{ie^5}{16\pi^2}\langle Q',\lambda'|\,\gamma_\mu\,|P',\lambda'\rangle G_{\lambda,\lambda'}(t')\times \\
& \langle Q,\lambda|\,\{\Gamma^{\mu}(t',{m_e}^2-\alpha,{m_e}^2)\;-\;\Gamma^{\mu}(t,{m_e}^2,{m_e}^2)\}\,|P,\lambda\rangle \qquad (6.12)\\
=\;& \frac{ie^5}{16\pi^2}\langle Q',\lambda'|\,\gamma_\mu\,|P',\lambda'\rangle G_{\lambda,\lambda'}(t')\langle Q,\lambda|\,\gamma^{\mu}\,|P,\lambda\rangle\,\{FF\;-\;FF^0\}\;- \\
& \frac{ie^5}{16\pi^2}\langle Q',\lambda'|\,\not{Q}\,|P',\lambda'\rangle G_{\lambda,\lambda'}(t')\langle Q,\lambda|\,\not{K}\,|P,\lambda\rangle\,\{FF_a\;+\;FF_b\} \\
=\;& \frac{ie^5}{16\pi^2}\langle Q',\lambda'|\,\gamma_\mu\,|P',\lambda'\rangle G_{\lambda,\lambda'}(t')\langle Q,\lambda|\,\gamma^{\mu}\,|P,\lambda\rangle\times \\
& \{-4+2B_0({m_e}^2-\alpha,m_0,m_e)-2B_0({m_0}^2,m_e,m_e)+3B_0(t,m_e,m_e) \\
& -3B_0(t',m_e,m_e)-\frac{3\alpha}{t'+\alpha}(B_0({m_e}^2-\alpha,m_0,m_e)-B_0(t',m_e,m_e))+ \\
& 2tC_0({m_e}^2,2{m_e}^2+t,{m_e}^2,m_0,m_e,m_e)- \\
& 2t'C_0({m_e}^2-\alpha,2{m_e}^2+t',{m_e}^2,m_0,m_e,m_e)\;\}\;- \\
& \frac{ie^5}{16\pi^2}\langle Q',\lambda'|\,\not{Q}\,|P',\lambda'\rangle G_{\lambda,\lambda'}(t')\langle Q,\lambda|\,\not{K}\,|P,\lambda\rangle\times \\
& \{-\frac{4t'}{t'+\alpha}C_0({m_e}^2-\alpha,2{m_e}^2+t',{m_e}^2,m_0,m_e,m_e)+ \\
& \frac{6t'-4\alpha}{(t'+\alpha)^2}B_0({m_e}^2-\alpha,m_0,m_e)-\frac{10t'}{(t'+\alpha)^2}B_0(t',m_e,m_e) \\
& +\frac{4}{t'+\alpha}\,(\frac{3}{2}\;+\;B_0({m_0}^2,m_e,m_e))\;\} \qquad (6.13)
\end{aligned}$$

The scalar integrals were written in explicit form in 6.13 since the FORM notation differs between the form-factor and internal emission routines. It is pivotal

for the consistency check that Eq. 6.13 be compared to the FORM output after replacing $\not{q} \rightarrow \not{K}$, which was done in the a3.gauge routine. The result reads, Ref. [24]:

$$\begin{aligned} A_3^{long} &= \frac{ie^5}{16\pi^2}\langle Q',\lambda'|\,\gamma_\mu\,|P',\lambda'\rangle G_{\lambda,\lambda'}(t')\langle Q,\lambda|\,\gamma^\mu\,|P,\lambda\rangle \times \\ &\left\{2tC_{124} - 2t'C_{134}^{\alpha} - 2B_{12} + 3B_{24} + \frac{2t'-\alpha}{t'+\alpha}B_{13}^{\alpha} - \frac{3t'}{t'+\alpha}B_{34}\right\} + \\ &\frac{ie^5}{16\pi^2}\langle Q',\lambda'|\not{Q}\,|P',\lambda'\rangle G_{\lambda,\lambda'}(t')\langle Q,\lambda|\not{K}\,|P,\lambda\rangle \times \\ &\left\{\frac{4t'}{t'+\alpha}C_{134}^{\alpha} + \frac{2}{t'+\alpha} - \frac{4}{t'+\alpha}B_{12} + \right. \\ &\left.\frac{10t'}{(t'+\alpha)^2}B_{34} + \frac{4\alpha-6t'}{(t'+\alpha)^2}B_{13}^{\alpha}\right\} \end{aligned} \tag{6.14}$$

Eq. 6.14 is expressed with the notation of scalar integrals given in section 3.3.1 and can be seen to be identical to the result in 6.13 by observing that $B_0(m_0^2, m_e, m_e) = B_0(m_e^2, m_0, m_e) - 2$. This therefore constitutes the strongest confirmation about the internal consistency of the calculation to this point since both results were derived in a completely independent manner!

The relation described by Eq. 6.12 is actually an example of a higher order Ward-Takahashi identity [19, 4]. This can be seen by following Feynman's treatment of gauge invariance [29], which leads to the following matrix identity [4] for the emission of a longitudinal photon from an internal part of the electron line with four-momentum P and possible dependence on other external momenta q_i:

$$K_\mu \Lambda^\mu(P, K, q_i) = \Gamma(P-K, q_i) - \Gamma(P, q_i) \tag{6.15}$$

The Γ-factors for non-zero transfer are directly related to self-energy expressions and can be obtained from graphs 3.6, 3.4 and 3.12 by removing the virtual photon connecting the two fermion lines. Thus, Eqs. 6.12 and 6.15 are two equivalent representations of the Ward-Takahashi identity. The Ward-identity for zero transfer will now be discussed in the following section.

6.3 Ward Identity

Symmetries play important roles in physical theories not only because they allow for an elegant and insightful mathematical formulation of physics but also because they impose stringent conditions on the possible states of a system or on relations between certain quantities of the theory. One important consequence of the gauge symmetry in QED is the Ward identity [2]. Since it links self-energy and vertex functions in the limit of zero momentum transfer, the calculated expressions in the respective chapters should be related according to:

$$\Gamma^\mu(0,P^2,P^2) \;=\; -\frac{\partial\Sigma(P,m_0,m_e)}{\partial P_\mu} \tag{6.16}$$

The l.h.s. of Eq. 6.16 can be derived by using the full result of Eq. 3.21 with both fermion legs off-shell and for zero transfer. This was done in the FORM routine *ffward* in the appendix Ref. [24], and gives:

$$\begin{aligned}\Gamma^\mu(0,P^2,P^2) \;&=\; (B_0(P^2,m_0,m_e) - B_0(m_0^2,m_e,m_e) - 4m_e^2C_{1230} - 5)\gamma^\mu \\ &\quad -\frac{2}{P^2}P^\mu \not{P}\end{aligned} \tag{6.17}$$

In order to obtain the r.h.s. of Eq. 6.16 one has to use the result for $\Sigma(P,m_0,m_e)$ in 3.42. This leads to

$$\begin{aligned}-\frac{\partial\Sigma(P,m_0,m_e)}{\partial P_\mu} \;&=\; -(4m_e^2C_{1230} + B_0(m_e^2,m_0,m_e) - B_0(P^2,m_0,m_e) + 3)\gamma^\mu \\ &\quad + \frac{\partial B_0(P^2,m_0,m_e)}{\partial P_\mu}\not{P}\end{aligned} \tag{6.18}$$

With

$$\begin{aligned}&\frac{\partial B_0(P^2,m_0,m_e)}{\partial P_\mu} \\ &= \frac{1}{i\pi^2}\int d^4l \frac{\partial}{\partial P_\mu}\frac{1}{(l^2-m_0^2)((l+P)^2-m_e^2)+i\epsilon} \\ &= -\frac{2}{i\pi^2}\int d^4l \frac{l^\mu + P^\mu}{(l^2-m_0^2)((l+P)^2-m_e^2)^2+i\epsilon} \\ &= -\frac{4}{i\pi^2}\int d^4l \int_0^1 dx \frac{x(l^\mu+P^\mu)}{(l^2+2lPx - m_0^2(1-x)+(P^2-m_e^2)x+i\epsilon)^3}\end{aligned} \tag{6.19}$$

and using [42]

$$\begin{aligned}I_0 \;&=\; \int d^nl \frac{1}{(l^2+2lP+M^2+i\epsilon)^\lambda} = i(-\pi)^{\frac{n}{2}}\frac{\Gamma(\lambda-\frac{n}{2})}{\Gamma(\lambda)}\frac{1}{(M^2-P^2+i\epsilon)^{\lambda-\frac{n}{2}}} \\ I_1 \;&=\; \int d^nl \frac{l^\mu}{(l^2+2lP+M^2+i\epsilon)^\lambda} = -P^\mu\, I_0\end{aligned} \tag{6.20}$$

one finally gets

$$\frac{\partial B_0(P^2,m_0,m_e)}{\partial P_\mu} \;=\; 2P^\mu\int_0^1 dx \frac{-x^2+x}{P^2x^2-(P^2-m_e^2+m_0^2)x+m_0^2+i\epsilon}$$

$$= \frac{2P^\mu}{P^2}\int_0^1 dx\left\{-1+\frac{\frac{m_e{}^2}{P^2}x}{x^2-\frac{P^2-m_e{}^2+m_0{}^2}{P^2}x+\frac{m_0{}^2}{P^2}+i\epsilon}\right\}$$
$$= -\frac{2P^\mu}{P^2} \qquad (6.21)$$

up to $\mathcal{O}(\frac{m_e{}^2}{P^2})$. Inserting 6.21 into 6.18 and using the relation

$$B_0(m_e{}^2, m_0, m_e) \;=\; 2 \;+\; B_0(m_0{}^2, m_e, m_e)\;, \qquad (6.22)$$

which was already used in section 6.2, yields the identical result to Eq. 6.17. This proves that the Ward identity 6.16 is satisfied by the expressions for the self-energy and vertex functions, calculated in this work in completely independent ways!

Chapter 7

Monte Carlo Results

7.1 Finite Mass Effects

In the previous chapters only massless fermions were considered. For high energy processes, this is a very good approximation when $\frac{m^2}{-t} \ll 1$ as long as the radiated photon is not emitted in a direction parallel to one of the fermion directions. Within the context of the theory of multiple bremsstrahlung in gauge theories at high energies [26], a method was developed to incorporate finite mass effects into a description using massless fermion spinors [6]. This is especially necessary when running Monte Carlo simulations, where a bulk of events is generated in the low angle emission area of phase space and a wrong collinear limit would render numerical results meaningless. Following the CALKUL collaboration [5], the mass terms important in the collinear limit have the following general form in the single bremsstrahlung case:

$$\frac{d\sigma^m}{K^0 dK^0 d\Omega_K d\Omega_{e^+}} = \frac{(Q'^0)^2}{2^9\pi^5 ss'} |A^m|^2 , \tag{7.1}$$

with

$$|A^m|^2 = -\frac{e^2m^2}{(qk)^2} f^0(q-k, p_i) , \tag{7.2}$$

where the photon is radiated nearly parallel to q, and f^0 denotes the non radiative cross section, summed over all polarizations, with the original q replaced by $q-k$. In the case of Bhabha scattering the Born cross section is proportional to the following invariant summed matrix element squared [5]:

$$f^B_{e^-+e^+} = \frac{2e^4}{t^2}(s^2+u^2) \tag{7.3}$$

The complete non-radiative cross section for the $\mathcal{O}(\alpha^2)$ single bremsstrahlung mass corrections is then proportional to

$$f^0_{e^-+e^+} = (1+\frac{e^2}{4\pi^2}ff^0)f^B_{e^-+e^+} \tag{7.4}$$

with

$$\begin{aligned} ff^0(t) &\equiv FF^0(t) - 4\pi ReB(t) \\ &= -2 + 2ln\frac{-t}{m_e{}^2} \end{aligned} \tag{7.5}$$

From Eq. 7.2 it follows that, when summed over all fermion legs, the finite mass terms for the $\mathcal{O}(\alpha^2)$ single bremsstrahlung corrections are given by

$$\begin{aligned} |A^{m_e}_{e^-+e^+}|^2 = & -\frac{2e^6 m_e{}^2}{(PK)^2}\left[1+\frac{e^2}{4\pi^2}ff^0(-2PQ+2QK)\right] \times \\ & \frac{(2PP'-2P'K)^2+(-2PQ'+2Q'K)^2}{(-2PQ+2QK)^2} \\ & -\frac{2e^6 m_e{}^2}{(QK)^2}\left[1+\frac{e^2}{4\pi^2}ff^0(-2PQ-2PK)\right] \times \\ & \frac{(2QQ'+2Q'K)^2+(-2QP'-2P'K)^2}{(-2PQ-2PK)^2} \\ & -\frac{2e^6 m_e{}^2}{(P'K)^2}\left[1+\frac{e^2}{4\pi^2}ff^0(-2P'Q'+2Q'K)\right] \times \\ & \frac{(2PP'-2PK)^2+(-2QP'+2QK)^2}{(-2P'Q'+2Q'K)^2} \\ & -\frac{2e^6 m_e{}^2}{(Q'K)^2}\left[1+\frac{e^2}{4\pi^2}ff^0(-2P'Q'-2P'K)\right] \times \\ & \frac{(2QQ'+2QK)^2+(-2PQ'-2PK)^2}{(-2P'Q'-2P'K)^2} \end{aligned} \tag{7.6}$$

7.2 The Soft Limit

The soft limit of the exact $\mathcal{O}(\alpha^2)$ expression is determined by combining all helicity-independent(hi) terms of the result 4.3 multiplying the lower order amplitude. Doing this and using Eq. 3.65 and Ref. [22] gives the following:

$$\begin{aligned} A^{hi}_{e^-} &= \frac{e^2}{16\pi^2}\left\{-8-8m_e{}^2C^0_{123}-2(tC_{124}+t'C^0_{134})+6B_{12}-6B_{34}\right\}A^{TL}_{e^-} \\ &= \frac{e^2}{16\pi^2}\left\{-8+\frac{2\pi^2}{3}-ln^2\frac{-t}{m_e{}^2}-ln^2\frac{-t'}{m_e{}^2}+6ln\frac{-t'}{m_e{}^2}\right. \\ &\quad \left.+4ln\frac{-t}{m_e{}^2}ln\frac{m_0}{m_e}+4ln\frac{-t'}{m_e{}^2}ln\frac{m_0}{m_e}-8ln\frac{m_0}{m_e}\right\}A^{TL}_{e^-} \end{aligned} \tag{7.7}$$

Using the virtual YFS-IR function from Eq. 5.11 one gets

$$\begin{aligned} & A_{e^-}^{hi} - \alpha\,[Re\ B(t) + Re\ B(t')]\, A_{e^-}^{TL} \\ = & \frac{e^2}{16\pi^2}\left\{-4 + 5ln\frac{-t'}{m_e{}^2} - ln\frac{-t}{m_e{}^2}\right\} A_{e^-}^{TL} \end{aligned} \tag{7.8}$$

In the soft limit $t = t'$ so that

$$\begin{aligned} A_{e^-}^{sl} - 2\alpha Re\ B(t) A_{e^-}^{TL} &= \frac{e^2}{4\pi^2}\left\{-1 + ln\frac{-t}{m_e{}^2}\right\} A_{e^-}^{TL} \\ &= \frac{e^2}{8\pi^2}\, ff^0(t)\, A_{e^-}^{TL}\,, \end{aligned} \tag{7.9}$$

where ff^0 is given by Eq. 7.5. Taking into account that the cross section is proportional to $2Re\{A_{e^-}^{TL} * A_{e^-}^{*}\}$, the soft limit contains the identical form factor as the mass correction term in 7.5. This is another consequence from the YFS-theory discussed in chapter 5 which states that in the soft limit, the summed and averaged bremsstrahlung cross section factorizes into a soft part given by $\widetilde{S}(k)$, Eq. 5.7, and the lower order cross section, theorem 5.6.
It is useful in Eq. 7.8 to keep t and t' separately, since the formula holds also for large values of $k = \frac{E_\gamma}{E_{Beam}}$ as numerical results in Fig. 7.1 show. In order to compare Eq. 7.7 with the result obtained by Fadin et al. [43], one has to use the real YFS-IR function given in 5.12. This then leads to

$$\begin{aligned} & A_{e^-}^{hi} + \alpha\left[\widetilde{B}(t, E_{cut}) + \widetilde{B}(t', E_{cut})\right] A_{e^-}^{TL} \\ = & \frac{e^2}{8\pi^2}\left\{-4 + ln\frac{-t}{m_e{}^2}(2ln\Delta - lnx)\right. \\ & \left. + ln\frac{-t'}{m_e{}^2}(3 + 2ln\Delta) - 4ln\Delta + lnx\right\} A_{e^-}^{TL} \end{aligned} \tag{7.10}$$

with $x = \frac{E_Q}{E_P}$ and $\Delta = \frac{E_{cut}}{E_P}$ (in the cm-system $E_P = E_{Beam}$). Both Eq. 7.8 and 7.10 are normalized such that they multiply $\frac{\alpha}{\pi} d\sigma^{\mathcal{O}(\alpha)}$ as is the case in Ref. [43]. The difference to the formula given by Fadin et al. is $\frac{1}{4} + \frac{1}{2}ln^2 x$. All equations are valid for electron-line emission. The other line must be added analogously.

7.3 Leading Log Comparisons

At this point all the pieces needed for a Monte Carlo integration are calculated and checked on a differential level. It is now necessary to combine the various results and include the phase space factors in order to get a normalized differential cross section. Following the conventions of Ref. [2, 1], the expression for $d\sigma^{\mathcal{O}(\alpha+\alpha^2)}$ reads:

$$\frac{d\sigma^{\mathcal{O}(\alpha+\alpha^2)}}{K^0dK^0d\Omega_K d\Omega_{e+}} = \frac{(Q'^0)^2}{2^9\pi^5 ss'}\sum_{\rho,\lambda,\lambda'} Re\left\{\left(A_{e^-}^{TL} + A_{e^+}^{TL}\right)\left[A_{e^-}^{*} + A_{e^+}^{*}\right]\right\} + \frac{(Q'^0)^2}{2^{10}\pi^5 ss'}\sum_{\rho,\lambda,\lambda'}\left|A_{e^-}^{TL} + A_{e^+}^{TL}\right|^2 + \frac{d\sigma^m}{K^0dK^0d\Omega_K d\Omega_{e+}} \quad (7.11)$$

The amplitudes A_e are expressed in Eq. 4.3; it is assumed that all helicity degrees of freedom have been summed over and that the initial states were averaged. This cross section still contains the IR-mass divergent terms proportional to $ln\frac{m_0}{m_e}$, which are identical to those given in Eq. 7.7. Following the YFS-prescription of chapter 5, the normalized infrared regulated (reg) differential cross section for the exact result 4.3 is then given by:

$$\frac{d\sigma_{reg}^{\mathcal{O}(\alpha+\alpha^2)}}{K^0dK^0d\Omega_K d\Omega_{e+}} = \frac{d\sigma^{\mathcal{O}(\alpha+\alpha^2)}}{K^0dK^0d\Omega_K d\Omega_{e+}} - 2\alpha Re\left\{B(t) + B(t')\right\}\frac{d\sigma^{\mathcal{O}(\alpha)}}{K^0dK^0d\Omega_K d\Omega_{e+}} \quad (7.12)$$

An analytic five dimensional integration over 7.12 is extremely involved and beyond known calculational techniques. It is also desirable to be able to change to a given detector geometry and new experimental cutoff parameters without having to do a completely new calculation. Both of these difficulties can be overcome by using a Monte Carlo (MC) approach [41]. The algorithm implemented uses the method of weighting [41]. Events, i.e. sets of final state four-momenta, are generated at random, with a probability for each configuration to occur given by 7.12. Any experimental situation can then easily be simulated by throwing away those events that do not satisfy the experimental conditions. The generation of events can be accomplished by first generating "trial" events according to some approximate cross section $\frac{d\sigma_{approx}}{K^0dK^0d\Omega_K d\Omega_{e+}}$, and assigning to each trial event a weight

$$w = \left(\frac{d\sigma_{reg}^{\mathcal{O}(\alpha+\alpha^2)}}{K^0dK^0d\Omega_K d\Omega_{e+}}\right)\left(\frac{d\sigma_{approx}}{K^0dK^0d\Omega_K d\Omega_{e+}}\right)^{-1} \quad (7.13)$$

The exact event distribution is then realized by accepting the trial events with a probability proportional to w. From the above considerations it is clear that $\frac{d\sigma_{approx}}{K^0dK^0d\Omega_K d\Omega_{e+}}$ must be as simple as possible and that the method is only practical if the weights 7.13 do not fluctuate too wildly. The approximate cross section chosen here is the one suggested by F.A.Berends and R.Kleiss [7] and was implemented into Fortran by S.A.Yost. In order to be able to generate the phase space variables $K^0, \theta_K, \Phi_K, \theta_{e+}$ and Φ_{e+} , the integral over $d\sigma_{approx}$ has to be known and some cuts for these parameters have to be chosen. Here, the algorithm of Ref. [7] was used and the cuts correspond to the SICAL W-N acceptance [45].

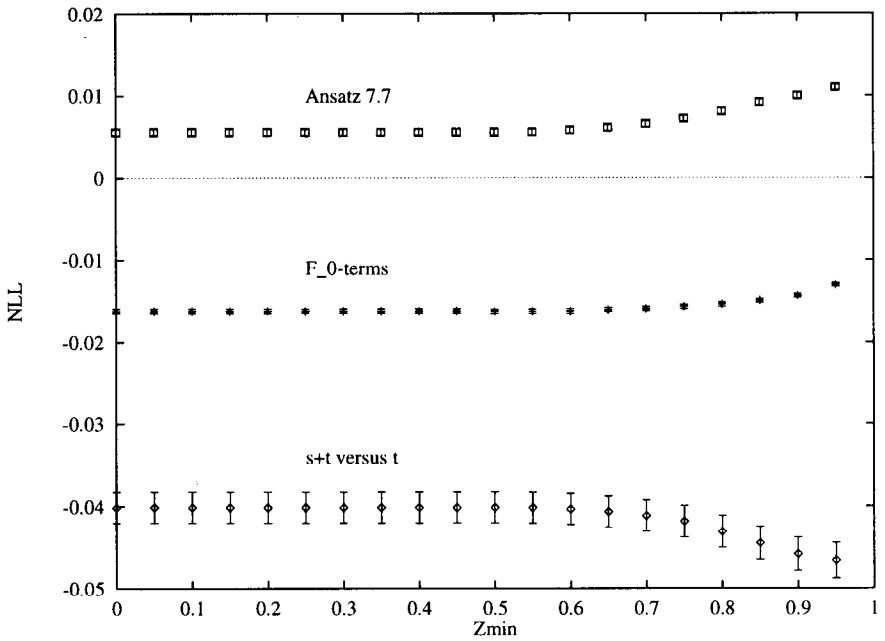

Figure 7.1: Results of a Monte Carlo integration corresponding to 10^5 events per point; $NLL \equiv \{\sigma^i_{reg} - \sigma^{\mathcal{O}(\alpha^2)}_{reg}\}/\sigma^{\mathcal{O}(\alpha^2)}_{reg}$ is a measure for the size of the subleading and pure $\left(\frac{\alpha}{\pi}\right)^2$ terms in the various cases (i). The real photon IR-singularity is regulated by a cutoff and cancels out of the ratios. The energy cut z_{min} is defined in Ref. [36], for example, as is the W-N acceptance.

The only practical way to calculate $\int w d\sigma_{approx}$ is to generate uniform distributions dq_i between $[0,1]$ for each differential factor and write:

$$d\sigma_{approx} = J dq_{K^0} dq_{\theta_K} dq_{\Phi_K} dq_{\theta_{e^+}} dq_{\Phi_{e^+}} , \tag{7.14}$$

where J is the Jacobian of the transformation 7.14. The integrated cross section is then given by summation of all accepted weights and averaging over the total number of generated events.

The results for the integrated exact $\mathcal{O}(\alpha^2)$ cross section are presented in Fig. 7.1 in comparison with several partial results following from the exact expression 4.3. It can be seen that the ansatz 7.7 stays within 1%(!) of the exact t-channel expression 4.3 for the chosen cuts. This is a remarkable result given the simplicity of that equation but should be seen as somewhat accidental, since many helicity dependent terms multiplying the tree-level amplitude apparently cancel, without any obvious physical necessity. Taking into account only $\mathcal{F}_0$ terms is also in excellent agreement with the complete t-channel result and remains within 2%. The effect of adding the s-channel, including Z-exchange, can be seen to be relatively small, roughly 5% of the second order single bremsstrahlung expression 4.3 for the chosen parameter space. In conclusion, for the accuracy

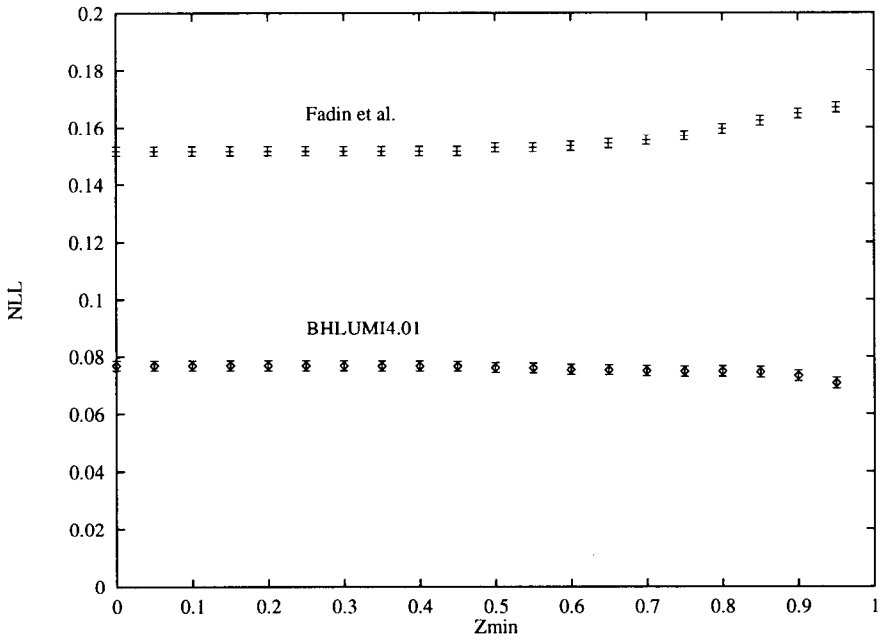

Figure 7.2: A comparison of the integrated cross section with two independent calculations, analogous to Fig. 7.1, corresponding to 10^5 events per point. The result 4.3, including s and t channel plus Z-exchange and IR-regularization, is seen to deviate in its non leading logarithmic parts from the pure t-channel expression given in Ref. [43] by up to 17%. The LL-ansatz implemented in BHLUMI4.01 [36] stays within 8% over the entire range of z_{min}.

required in the context of 0.1% precision radiative corrections, both t-channel approximations 7.7 and using only $\mathcal{F}_0$ terms in 4.3 represent perfectly acceptable approaches.

As a further consistency check and also as a measure for the size of the hitherto missing subleading terms from the second order single bremsstrahlung calculation, the complete result derived in this work with the s-channel and Z-exchange is compared in Fig. 7.2 to two independent leading log type results. The size of the overall subleading parts is very much dependent of what exactly is included in the leading log ansatz and the authors of Ref. [43] claim to have all terms contributing to a 0.1% precision level in their formula. While an exact value for the size of the missing subleading bremsstrahlung parts is difficult to specify, Fig. 7.2 suggests that the total contribution of those terms is below 20% of the total pure second order result. Since the size of the complete second order contribution is roughly 0.35% of the Born process for the W-N acceptance at SICAL [45], the subleading terms are found to be small but non negligible. The good agreement of the LL-ansatz in BHLUMI4.01, however, suggests that the accuracy of the theoretical precision level quoted in Refs. [35, 39, 40] as $\mathcal{O}(0.16\%)$ relative to the Born process, is rather conservative indeed.

Chapter 8

Conclusions

In this thesis, the sole outstanding contribution to low angle Bhabha scattering above the 0.1% precision level, the second order single bremsstrahlung subleading terms, have been calculated exactly, i.e. including pure $\left(\frac{\alpha}{\pi}\right)^2$ corrections. While other leading log and partial results have been published [8, 43], Eq. 4.3 represents the first complete, fully differential exact $\mathcal{O}(\alpha)$ corrections to $e^- + e^+ \longrightarrow e^- + e^+ + \gamma$ in the LEP/SLC energy regime. The accuracy of the presented result is well below 0.05%, which is the level required in order to have meaningful comparisons with measurements of the new luminosity detectors at LEP [3]. The calculated expression 4.3 has passed several strong internal consistency checks as well as analytical and numerical comparisons with leading log type results:

It was shown in chapter 5 that the expression for the internal emission amplitudes 3.56 is indeed UV-finite and possesses the expected logarithmic virtual photon mass dependence as predicted by the Yennie, Frautschi and Suura program.
Chapter 6 provided an essential link between technically completely unrelated parts of the calculation in deriving the gauge variation for the initial state internal emission graph 3.6 by replacing $\varepsilon^\mu \rightarrow K^\mu$ and comparing this with the analytical expressions for the on- and off-shell form factors. The demonstrated agreement represents a Ward-Takahashi identity for non-zero momentum transfer. In addition to being a very strong check on the internal emission result, it also demonstrates the correct application of the on-shell renormalization scheme employed in this work. In section 6.3, the other remaining part of the calculation, the self-energy contribution, was linked to the off-shell form factor in the limit of zero transfer. The verified Ward identity completes the full circle of all the various terms given in this thesis and establishes powerful evidence for the overall correctness of the derived expressions.
In chapter 7 the mass corrections showing a double pole structure, the only relevant mass terms in the high energy approximation for a Monte Carlo integration, were derived and subsequently added to yield the complete result. The

soft limit of Eq. 4.3 was given explicitly in differential form in 7.9 and shown to be connected to the lower order cross section according to YFS-theory. By combining all helicity independent terms, an approximate formula 7.7 was found that shows agreement with the exact result within 1%(!) after a Monte Carlo phase space integration for SICAL-type cuts. It was also shown that the terms proportional to the tree-level cross section make up for roughly 98% of the second order t-channel contribution and thus contain all relevant leading and subleading logarithmic corrections. The size of the s-channel corrections including Z-exchange was found to be as small as expected, around 5% relative to the pure t-channel result. Further MC results demonstrated that the exact expression 4.3 relates to other leading log type calculations as follows:

The IR−regulated ratios $\{\sigma^i_{reg} - \sigma^{\mathcal{O}(\alpha^2)}_{reg}\}/\sigma^{\mathcal{O}(\alpha^2)}_{reg}$, which are a measure of the size of the missing subleading terms in the various partial results (i), revealed that the calculation by Fadin et al. lies within 17% of the exact formula 4.3. It was furthermore shown that the ansatz used in BHLUMI4.01 [35] is within 8% of the answer derived in this work for the specified cuts. Since the size of the $\mathcal{O}(\alpha^2)$ single bremsstrahlung contribution is of the order of 0.35% relative to the Born process for cuts chosen to correspond to the experimental luminosity detector SICAL at ALEPH, this will have important consequences for the overall level of precision of BHLUMI4.x. While several questions about the dependence on experimental cuts for the above agreement as well as those relating to the technical precision domain remain to be discussed more thoroughly [38, 37], it is safe to assume that the precision of BHLUMI4.x will be below the $1pm$ level.

In light of the results presented in this thesis, it will soon be realistic to achieve a theoretical level of accuracy below $1pm$ for the total cross section in low angle Bhabha scattering. Together with high precision measurements of second generation luminosity detectors at CERN, it will hopefully be possible to determine various electroweak parameters in a way that sets stringent conditions on the range of validity of this theory and, simultaneously, to open up a new regime in the search for physics beyond the Standard Model.

Acknowledgments

I would like to thank B.F.L. Ward for suggesting this project for my doctoral thesis as well as his support throughout its duration. By the same token I am obliged to S.A. Jost for the abovementioned contributions and likewise to S. Jadach. In addition, my gratitude extends to H.D. Dahmen for his support of my doctoral thesis from abroad. Finally, I am grateful to S.J. Brodsky and the SLAC-theory group for their kind hospitality.

Bibliography

[1] Bjorken, Drell. Relativistic quantum fields. *McGraw-Hill Book Company*, 1964.

[2] Bjorken, Drell. Relativistic quantum mechanics. *McGraw-Hill Book Company*, 1964.

[3] B.Pietrzyk. *Proceedings of the Tennessee International Symposium on Radiative Corrections, Gatlinburg U.S.A.*, Edited by B.F.L.Ward:page 138, 1994.

[4] D.R.Yennie, S.C.Frautschi, H.Suura. *Annals of Physics*, 13:379, 1961.

[5] F.A.Berends, P.De Causmaecker, R.Gastmans, R.Kleiss, W.Troost, T.T.Wu. *Nuclear Physics*, B206:61, 1982.

[6] F.A.Berends, P.De Causmaecker, R.Gastmans, R.Kleiss, W.Troost, T.T.Wu. *Nuclear Physics*, B239:382, 1984.

[7] F.A.Berends, R.Kleiss. *Nuclear Physics*, B228:537, 1983.

[8] F.A.Berends, W.L.Van Neerven, G.J.H.Burgers. *Nuclear Physics*, B297:429, 1987.

[9] F.Bloch, A.Nordsieck. *Phys.Rev.*, 52:54, 1937.

[10] G.Altarelli. *CERN-TH/95-3*, 1995.

[11] Gastmans, Wu. The ubiquitous photon. *Oxford Sience Publications*, 1990.

[12] G.J.Oldenborgh. ff, a package to evaluate one-loop feynman diagrams. NIKHEF-H/90-15, 1990.

[13] G.J.van Oldenborgh, J.A.M.Vermaseren. *Zeitschrift fuer Physik*, C46:425, 1990.

[14] Gradshteyn, Ryzhik. Table of integrals, series and products. *Academic Press*, 1994.

[15] Green,Schwarz,Witten. Superstring theory, vol.1. *Cambridge University Press*, 1987.

[16] G.'t Hooft. *Nucl.Phys.*, B33:173, 1971.

[17] G.'t Hooft, M.Veltman. *Nuclear Physics*, B153:365, 1979.

[18] H.J.Bhabha. *Proc.Roy.Soc.(London)*, A154:195, 1935.

[19] Itzykson, Zuber. Quantum field theory. *McGraw-Hill Book Company*, 1980.

[20] J.Steinberger. *Phys.Rep. 203 and references therein*, page 345, 1991.

[21] L.H.Ryder. Quantum field theory. *Cambridge University Press*, 1985.

[22] M.Boehm, H.Spiesberger, W.Hollik. *Fortschritte der Physik*, 34:687, 1986.

[23] M.Kaku. Quantum field theory. *Oxford University Press*, 1993.

[24] M.Melles. Doctoral thesis. *Siegen University*, Nov. 1995.

[25] P.De Causmaecker, R.Gastmans, W.Troost, T.T.Wu. *Physics Letters*, 105B:215, 1981.

[26] P.De Causmaecker, R.Gastmans, W.Troost, T.T.Wu. *Nuclear Physics*, B206:53, 1982.

[27] P.Ramond. Field theory. *Addison-Wesley Publishing Company, Inc.*, 1990.

[28] R.Kleiss and S.van der Marck. *Nuclear Physics*, B342:61, 1990.

[29] R.P.Feynman. *Phys.Rev.*, 76:769, 1949.

[30] R.P.Feynman. Quantum electrodynamics. *The Benjamin/Cummings Publishing Company, Inc.*, 1962.

[31] S.Dittmaier. *BI-TP 93/61*, 1993.

[32] S.Jadach. *Talk at the Physics Seminar of the Univ. of TN and private communication*, 1994.

[33] S.Jadach, B.F.L.Ward. *Phys.Rev.*, D38:2897, 1988.

[34] S.Jadach, E.Richter-Was, B.F.L.Ward, Z.Was. *Computer Physics Communications*, 70:305, 1992.

[35] S.Jadach, E.Richter-Was, B.F.L.Ward, Z.Was. *CERN-TH/95-38*, 1995.

[36] S.Jadach, E.Richter-Was, B.F.L.Ward, Z.Was. preprint. *CERN-TH-95-38*, in press at Phys.lett.B, 1995.

[37] S.Jadach, M.Melles, B.F.L.Ward, S.A.Yost. *In preparation.*

[38] S.Jadach, M.Melles, B.F.L.Ward, S.A.Yost. *submitted to Physics Letters B*, 1995.

[39] S.Jadach, M.Melles, W.Placzek, E.Richter-Was, M.Skrzypek, B.F.L.Ward, Z.Was, S.A.Yost. *Proceedings of the Tennessee International Symposium on Radiative Corrections, Gatlinburg U.S.A.*, World Scientific, Edited by B.F.L.Ward:153, 1994.

[40] S.Jadach, M.Melles, W.Placzek, E.Richter-Was, M.Skrzypek, B.F.L.Ward, Z.Was, S.A.Yost. *CERN Yellow Report 95-03, Reports of the working group on precision calculations for the Z resonance*, Edited by D.Bardin, W.Hollik, G.Passarino:343, 1995.

[41] Sobol. The monte carlo method. *The University of Chicago Press*, 1974.

[42] S.Pokorski. Gauge field theories. *Cambridge University Press*, 1987.

[43] V.Fadin, E.A.Kuraev, L.Lipatov, N.P.Merenkov, L.Trentadue. *Proceedings of the Tennessee International Symposium on Radiative Corrections, Gatlinburg U.S.A.*, Edited by B.F.L.Ward:168, 1994.

[44] W.Beenakker, B.Pietrzyk. *Physics Letters*, B296:241, 1992.

[45] W.Beenakker, B.Pietrzyk. *Physics Letters*, B304:366, 1993.

[46] Z.Xu, D.H.Zhang, L.Chang. *Nucl.Phys.*, B291:392, 1987.